NASA Contractor Report 172237

MATERIAL CHARACTERIZATION OF STRUCTURAL ADHESIVES IN THE LAP SHEAR MODE

Steven C. Schenck and Erol Sancaktar

CLARKSON COLLEGE OF TECHNOLOGY
Potsdam, New York 13676

Grant NAG1-284
September 1983

National Aeronautics and
Space Administration

Langley Research Center
Hampton, Virginia 23665

ACKNOWLEDGMENTS

This project was sponsored by NASA's Langley Research Center under the NASA Grant NAG-1-284. Dr. William S. Johnson was the NASA technical monitor and his assistance is gratefully acknowledged. Thanks are also due to Dr. Terry L. St. Clair of NASA Langley for his friendly guidance and assistance throughout the implementation of this project.

This work constituted Steven C. Schenck's M.S. Thesis.

NOMENCLATURE

A,B,C	material constants for Maxwell model
A',B',C'	material constants
A'',B'',C''	material constants for Kelvin model
a_T, b_T, c_T	functions of temperature
G	shear elastic modulus
$H(t)$	unit step function
K,n	material constants
R	universal gas constant
t_o	time constant
t_r	rupture time
T	absolute temperature
U_o	constant activation energy per mole
$\gamma,\dot{\gamma}$	one dimensional shear strain and shear strain rate
$\varepsilon_{ij}^E, \varepsilon_{ij}^V$	elastic and viscoelastic strains
θ	elastic limit stress
μ	coefficient of viscosity in shear
$\tau,\dot{\tau}$	one dimensional shear stress and shear stress rate
τ_{ult}	ultimate shear stress
τ_o	level of constant stress
$\tau',\tau'',\dot{\gamma}'$	material constants
$\tau(t)$	time dependent shear stress
ϕ	elastic limit shear strain
χ	time dependent material property
γ_o	level of initial (instantaneous) strain in a creep test
ν	Poisson's ratio

LIST OF FIGURES

LIST OF TABLES

CHAPTER 1

INTRODUCTION

Structural adhesives are preferred over the customary penetration techniques for joining of modern lightweight-composite materials. Their usage increased considerably during the last decade in the aerospace, automotive, naval, and many other industries. Structural adhesives are superior to conventional means of joining materials because of their flexibility and toughness, lightness of weight, exceptional thermal stability, solvent and moisture resistance, and excellent mechanical properties at room and elevated temperatures.

In joining mechanical components, the structural adhesive and mode of bonding (i.e. lap, butt, scarf, etc.) to be used is usually determined by in- service requirements. Single lap joints are widely used due to their applicability in many industrial designs.

In the absence of catastrophic crack propagations, the failure of lap joints may occur in one of the following modes:

1) Rupture of the adhesive layer, when the ultimate stress is reached;

2) Creep rupture of the adhesive layer when a high level of constant load is used;

3) Failure of the adherends.

Failure in the third mode will be unlikely when metal adherends such as steel or titanium are used. It is necessary, however, to consider the first two modes of failure for the design of adhesively bonded joints.

For design purposes, one often needs only the elastic properties

(namely Young's modulus and elastic limit stress) and failure stresses as a function of rate, time and temperature. If such is the case, then a satisfactory characterization can be obtained with the use of a semi-empirical approach to describe the failure stresses as a function of rate and temperature for constant strain rate loading and as a function of time and temperature for constant load conditions. This approach assumes that the viscoelastic effects are negligible in the initial portion of the stress-strain curve, so that an initial elastic strain rate can be defined. Previous work on a variety of polymeric materials and adhesives proved this assumption to be a valid one [1, 2, 3, 4, 5].

If information on the magnitude of strains (passed the elastic limit) is also required, then one needs to use a theoretical approach with the application of a mechanical model to characterize the material. Information on failure stresses can be extracted from such an approach if perfectly plastic flow is present (i.e. if the constant strain rate stress-strain curve has an asymptote). However, one still needs to use semi-empirical methods associated with the model, to obtain the creep rupture stresses. Furthermore, the use of a semi-empirical method is necessary to obtain rupture stresses for constant strain rate conditions, when perfectly plastic flow is not present.

It should also be noted that for some linear thermoplastic adhesives the effects of rate on the failure stresses may be negligible enough to permit the use of a nonlinear elastic relation to characterize the constant strain rate stress-strain behavior.

The semi-empirical relation proposed to describe rupture stresses

at room and elevated temperatures are Ludwik's equation [6] for the constant strain rate condition and Zhurkov's [7] and Crochet's [8] equations for the creep condition. It should be noted that the original form of Ludwik's and Crochet's equations do not include thermal effects. This report proposes an empirical modification of Ludwik's equation and an empirical extension of Crochet's equation to describe the effects of temperature.

Literature Review

The strength of adhesively bonded joints are known to depend on rate, time and temperature. H. F. Brinson [1] demonstrated that yielding in polycarbonate is both rate and time dependent. H. F. Brinson et. al. [2] studied the stress-strain and rate and time dependent yield behavior of Metlbond adhesive in the bulk form. Uniaxial tensile constant strain rate, creep and relaxation tests were performed for this purpose. According to Brinson, the rate dependent variation of the linear elastic limit and the failure stresses for the bulk adhesive could be described with a semi-empirical equation proposed by Ludwik [6], whereas time dependent variation of yielding could be correlated with a delayed yield equation proposed by Crochet [8]. Furthermore, the modified Bingham model was shown to represent adequately the constant strain rate stress-strain behavior of the bulk adhesive. The same model was later used by Sancaktar [3] for characterizing the viscoelastic shear behavior of a structural adhesive in the bulk and bonded forms.

Sancaktar and Padgilwar [5] studied the rate and time dependent mechanical behavior of LARC-3 adhesive in the lap shear mode by using

constant strain rate and creep tests. The constant strain rate stress-strain curves of LARC-3 contained regions of elastic behavior followed by regions of viscoplastic behavior. Maximum and elastic limit shear stresses were shown to be rate dependent and their variations with the initial elastic strain rate agreed well with the semi-empirical equation proposed by Ludwik [6]. A creep to failure phenomenon was shown to exist and was correlated with the delayed yield equation proposed by Crochet [8]. Analytical predictions based on the Chase-Goldsmith model [4] were shown to agree well with the experimental stress-strain-strain rate data.

Temperature also has a strong influence on the mechanical stress-strain properties of adhesives. For instance, the effects of temperature on the strength of lap shear specimens bonded with a high molecular weight thermoplastic adhesive have been investigated by Bugel, Norwalk and Snedeker [9]. They reported a sharp decrease in the joint strength for temperatures above 160°F (71°C).

Some mechanical data on the Thermoplastic Polyimidesulfone adhesive is available in a paper by St. Clair and Yamaki [10]. They report that the lap shear strength decreased from 4150 psi (28.6 MPa) to 2620 psi (18.1 MPa) when the test temperature was increased from the room condition to 450°F (232°C). St. Clair and Yamaki also report that thermal aging of the adhesive in the bonded form at temperatures up to 450°F (232°C) resulted in a reduced lap shear strength. For example, the ambient temperature strength of lap shear specimens that had been aged for 5000 hours at 450°F (232°C) was 3640 psi (25.1 MPa), while the same strength for the unaged specimens was 4150 psi (28.6 MPa).

Adhesive manufacturers generally do not supply detailed information on the rate, time and temperature dependent variation of the lap shear properties. When data is available, it is usually limited to the ultimate strength values.

Experimentally measured lap joint strength values for Thermoplastic Polyimidesulfone, FM 73 and FM 300 adhesives are available in the literature [10, 11, 12]. Information in regard to the rate, time and temperature dependent single lap mechanical behavior for these three adhesives, however, is yet to be obtained during this investigation.

The present investigation uses single lap specimens which were supplied by the NASA Langley Research Center. For such specimens the shear stresses are calculated as load divided by the overlap area, as prescribed by the ASTM standards. It should be noted, however, that the shear stresses calculated in this manner provide only approximate values as the actual shear stress distribution along the overlap area is not uniform but in fact is part of a biaxial stress state. The exact form of the stress distribution in single lap joints has been described by Goland and Reissner [13].

Objective

The purpose of the current investigation was to find a practical method for characterizing structural adhesives in the bonded lap shear mode. The applicability of the proposed characterization method was to be assessed by:

1) obtaining experimental data on the delayed failure(creep to yield) behavior of three different model adhesives in the bonded

form at both room and elevated temperatures;

2) obtaining experimental data on the constant strain rate shear stress-strain behavior of three different model adhesives in the bonded form at both room and elevated temperatures;

3) developing or identifying viscoelastic or nonlinear elastic models which will describe the mechanical behavior observed in the above mentioned experimental data;

4) determining whether Crochet's equation will describe the delayed failure behavior observed in experiments;

5) assessing the applicability of Zhurkov's (modified) equation in describing the time and temperature dependent behavior of failure stresses under constant loading conditions;

6) determining whether Ludwik's equation will describe the rate dependency of rupture stresses and elastic limit stresses and strains.

The three model adhesives, one of which was developed at the NASA Langley Research Center, were applied on titanium adherends in the form of single lap joints to represent in-service conditions. The adhesives are:

1) Thermoplastic Polyimidesulfone

2) FM 73, and

3) FM 300 adhesives.

1) Thermoplastic Polyimidesulfone is a novel adhesive developed at NASA - Langley Research Center. It has thermoplastic properties and solvent resistance. It is processable in the 482 - 662 F^{o}(250 - 350^{o}C) range and has high temperature resistance [10].

2) FM 73 is a modified epoxy adhesive film with carrier cloth. It is manufactured by the American Cyanamid Company. Its product information brochure reports a service temperature range of -67°F to 248°F (-55°C to 120°C) with high moisture resistance [11].
3) FM 300 is a modified epoxy adhesive film supplied with a "tricot - knit" carrier cloth that offers a good mixture of structural and handling properties. It is manufactured by the American Cyanamid Company as a supported film. Its product information brochure reports a service range of -67°F to 300°F (-55°C to 150°C) with excellent moisture and corrosion resistance [12].

The second chapter of this report is devoted to the analytical description of adhesive mechanical behavior with the presentation of constitutive equations and their solutions for constant strain rate and load conditions.

Chapter 3 outlines the experimental procedure. Materials selected for the study and specimen features are reviewed.

Chapter 4 is devoted to the discussion of the results. Theoretical results obtained from the proposed constitutive equations are compared with the experimental data.

The final chapter presents the conclusions.

CHAPTER 2

ANALYTICAL CONSIDERATIONS

In designing single lap joints bonded with a viscoelastic adhesive, a complete material characterization of the adhesive is needed. Such a characterization usually includes the elastic properties (namely Young's Modulus and elastic limit stress) and the failure stresses as a function of strain rate, time and temperature. A satisfactory characterization can be obtained by describing the rupture stresses as a function of rate under constant strain rate loading and as a function of time and temperature under constant loading by using a semi-empirical approach. In this approach, the rate dependency of the rupture stresses under constant strain rate loading can be expressed with the semi-empirical equation proposed for metals by Ludwik (as reported by Thorkildsen [6]) in the form

$$\tau_{ult} = \tau' + \tau'' \text{ Log } \left(\frac{\dot{\gamma}}{\dot{\gamma}'_o}\right) , \tag{1}$$

where τ_{ult} is the ultimate shear stress, $\dot{\gamma}_o$ is the initial elastic shear strain rate and τ', τ'' and $\dot{\gamma}'_o$ are material constants. This equation was used successfully by Brinson et. al. [1,2,3] and Sancaktar [5] in describing the rate dependence of rupture stresses for many polymeric materials in the bulk tensile shear, and bonded lap shear modes.

The same form of equation (1) can also be used to describe the variation of elastic limit shear stresses and strains with initial elastic shear strain rates. These expressions may be written as

$$\theta = \theta' + \theta'' \text{ Log}(\dot{\gamma}/\dot{\gamma}') \tag{2}$$

$$\phi = \phi' + \phi'' \text{ Log}(\dot{\gamma}/\dot{\gamma}') \tag{3}$$

where additional material constants are defined accordingly.

Superposition of temperature effects on equations (1), (2) and (3) would require experimental justification. For example, examination of rate vs. strength data for copper [15] at various temperatures ($73^{\circ}F < T < 1832^{\circ}F$, $23^{\circ}C < T < 1000^{\circ}C$) indicates a near parallel shift in the strain rate vs. strength relation particularly in the $392^{\circ}F$ ($200^{\circ}C$) to $1472^{\circ}F$ ($800^{\circ}C$) region. Such a parallel shift in equations (1), (2) and (3) could be expressed as

$$\tau_{ult} = \{a_T\}[\tau'] + \tau'' \text{ Log } (\dot{\gamma}/\dot{\gamma}') \tag{4}$$

$$\theta = \{b_T\}[\theta'] + \theta'' \text{ Log } (\dot{\gamma}/\dot{\gamma}') \tag{5}$$

$$\phi = \{c_T\}[\phi'] + \phi'' \text{ Log } (\dot{\gamma}/\dot{\gamma}') \tag{6}$$

where a_T, b_T and c_T are functions of temperature.

Temperature dependent delayed failure of structural adhesives can be described with the use of Zhurkov's and/or Crochet's creep-rupture equations. The modified (by Slonimskii [16]) form of Zhurkov's creep-rupture equation is given by:

$$t_r = t_o \exp \left[\frac{U_o}{RT} - \gamma\sigma\right] \tag{7}$$

where

t_r = rupture time

t_0 = a constant normally about 10^{-12} (stated to be the period of natural oscillation)

U_0 = a constant activation energy per mole (associated as an energy-barrier term)

γ = a constant

σ = applied uniaxial stress

R = universal gas constant

T = absolute temperature.

This equation was recently used by Brinson et. al. to describe the creep-rupture behavior of various polymer-matrix composites [17].

A decaying exponential relation of the form

$$\sigma(t) = A' + B' \exp(-C'\chi) \tag{8}$$

was proposed by Crochet to describe delayed failures. In equation (8), $\sigma(t)$ is the time dependent maximum stress, A', B' and C' are material constants and X is a time dependent material property given by

$$\chi = [(\varepsilon_{ij}^V - \varepsilon_{ij}^E)(\varepsilon_{ij}^V - \varepsilon_{ij}^E)]^{\frac{1}{2}} \tag{9}$$

where ε_{ij}^V and ε_{ij}^E refer to viscoelastic and elastic strains, respectively. Equation (8) can be interpreted for the pure shear condition. Use of a viscoelastic model is necessary, however, in order to obtain the material property X. For practical purposes,

simple linear viscoelastic models, Maxwell fluid or Kelvin solid can be used to facilitate the solution to equation (9). The use of Maxwell model results in

$$\tau(t) = A + B \exp\left[-\frac{C\tau_o}{\mu} t\right] \quad (10)$$

and the use of Kelvin model results in

$$\tau(t) = A'' + B'' \exp\left[C'' e^{-\frac{G}{\mu} t}\right] \quad (11)$$

where:

$\tau(t)$ = time dependent maximum shear (rupture) stress

τ_o = level of constant stress,

μ = coefficient of viscosity in shear

G = modulus of elasticity in shear

Apparently equation (11) describes a much faster approach in time of the rupture stresses to their asymptotic values.

The asymptotic values A and (A"+B") of equations (10) and (11) respectively, are important design parameters, as they represent the maximum safe stress values below which creep failures are not expected to occur. One can express A and/or (A"+B") values as a function of the applied temperature to represent experimental data in an empirical fashion.

In order to predict the stress-strain behavior of the adhesive and to extract failure information for constant strain rate and constant stress modes, one needs to determine the viscoelastic model which will describe the material adequately. If the rate effects on

the material are determined to be negligible, then the use of a nonlinear elastic relation may also be adequate. Brinson et. al. [1] used the modified Bingham model (shown in Figure 2), which was modified from the Schwedoff model [18], for characterizing the tensile behavior of Metlbond adhesive. The modified Bingham model was later used by Sancaktar [3] for characterizing the shear behavior of the same adhesive. For that work, the modified Bingham model was applied in the form,

$$\begin{aligned} \tau &= G\,\gamma && \tau \leq \theta \\ \dot{\gamma} &= \frac{\dot{\tau}}{G} + \frac{\tau-\theta}{\mu} && \theta < \tau \leq \tau_{ult} \end{aligned} \tag{12}$$

where τ and γ are shear stress and strain respectively, and θ is the elastic limit shear stress.

To obtain the constant strain rate relation, the above constitutive equation is solved according to the condition

$$\dot{\gamma} = R = \text{constant} \tag{13}$$

to result in

$$\tau = G\,\gamma \qquad \tau \leq \theta, \tag{14}$$

$$\tau = \theta + \mu\,\dot{\gamma}\left[1 - \exp^{-\frac{(\gamma-\phi)G}{\mu\,\dot{\gamma}}}\right] \qquad \theta < \tau \leq \tau_{ult} \tag{15}$$

where ϕ is the elastic limit strain.

The creep relation is obtained by using a step loading

$$\tau(t) = \tau_o H(t) \tag{16}$$

where H(t) represents the unit step function and τ_o is the level of constant stress, with the initial condition

$$\gamma(t=o) = \frac{\tau_o}{G_o} \tag{17}$$

to obtain

$$\gamma(t) = \frac{\tau_o - \theta}{\mu} t + \frac{\tau_o}{G} \quad . \tag{18}$$

In order to extract creep-rupture information from the given model, Crochet's delayed failure equation (equation 8) is used. Equations (8) and (9) can be applied to the shear condition by subtracting the elastic strain

$$\gamma_o = \tau_o / G_o \tag{19}$$

from the model's creep equation (equation 18), to obtain χ and substituting into equation (8) to result in

$$\tau(t) = A + B \exp\,[-K(\tau(t)-\theta)t] \; . \tag{20}$$

Equation (20) is the creep-rupture equation based on the modified Bingham model. It should be noted that the time-temperature superposition principle can be used along with equation (20) to make

it useful at different temperature levels. Naturally, it is not expected that the modified Bingham model will characterize all available adhesives. One can, however, use other viscoelastic models and follow the procedure described above to characterize most adhesives. Some examples of such application would be the use of the Chase-Goldsmith model by Sancaktar [5] to characterize LARC-3 adhesive in the bonded form and the use of Schapery's nonlinear constitutive equation [19] by Brinson et. al. [20] to characterize SMC-25 fiber reinforced polyester composite.

If the rate effects on adhesive behavior is determined to be weak, then a nonlinear elastic relation can be used to fit the stress-strain data. The power function relation expressed for the state of pure shear in the form:

$$\tau = K \gamma^n \tag{21}$$

where K and n are material constants, is proposed for this purpose.

CHAPTER 3

EXPERIMENTAL PROCEDURES

Materials and Specimen Features

The processing of the test specimens bonded with Thermoplastic Polyimidesulfone has been described in detail by St. Clair [10]. Two one-inch (2.54 cm) wide, 0.05 inch (0.127 cm) thick titanium alloy strips which are exact copies of each other are sand blasted with aluminum oxide of 120 mesh. These duplicate strips are then coated with poly (amide-acid sulfone) which is formed by mixing 0.0569 lbs (25.8 gms) of 3,3',4,4'-Benzophenonetetracarboxylic dianhydride(BTDA) in a solution made up of 0.0439 lbs (19.9 gms) of 3,3'-diaminodiphenylsulfone(3,3'-DDS) in 0.5701 lbs (258.6 gms) of bis (2-methoxyethyl) ether. Fifteen minutes of thermal treatments at 212 ^{o}F (100 ^{o}C) and 392 ^{o}F (200 ^{o}C), respectively, are applied to convert the amide-acid to the amide by removing the solvent. The adhesive layers are then applied onto the adherend strips. A 0.004 inch (0.010 cm) thick piece of woven glass cloth is inserted between the strips to control the adhesive thickness. A pressure of 200 psi (1.38 MPa) is applied and the specimen heated at a rate of 9 ^{o}F/min (5 ^{o}C/min) up to 572 ^{o}F (300 ^{o}C). The bonded specimen is then cooled and removed.

The adhesive, FM 73, is a modified epoxy adhesive film with a polyester knit fabric that offers optimum physical properties. It is manufactured by the American Cyanamid Company. Its product information brochure reports a service range of -67 ^{o}F to 248 ^{o}F (-55 ^{o}C to 120 ^{o}C) with a high resistance to moisture.

The bonding procedure with FM 73 adhesive is described in detail

by its product information brochure [11]. Two duplicate one-inch (2.54 cm) wide, 0.05 inch (0.127 cm) thick titanium alloy strips are cleaned and dried to provide a grease-free surface for bonding. Patterns of FM 73 adhesive film are cut and the adhesive's protective covering is peeled off at room temperature. The adhesive film is applied smoothly on the duplicate titanium strips at approximately 110 °F (43 °C) to provide additional tacking. Curing of the joint is done by first heating it up to 250°F (121°C) at a rate of approximately 6 °F/min (3.3°C/min). At the temperature of 250°F (121°C) a pressure of 40 psi (276 kPa) is applied for 60 minutes. The bonded specimen is then cooled and removed.

The adhesive, FM 300, is a modified epoxy adhesive film supplied with a "tricot-knit" carrier cloth that offers a good mixture of structural and handling properties. It is manufactured by the American Cyanamid Company as a supported film. Its product information brochure reports a service range of -67°F to 300°F (-55°C to 150°C) with excellent moisture and corrosion resistance.

The bonding procedure with FM 300 adhesive is described in detail by its product information brochure [12]. Two duplicate one-inch (2.54 cm) wide, 0.05 inch (0.127 cm) thick titanium alloy strips are cleaned and dried to provide a grease-free surface for bonding. Patterns of FM 300 adhesive film are cut and the adhesive's protective covering is peeled off at room temperature. The adhesive film is then applied smoothly on the duplicate titanium strips. Curing of the joint is done by first heating it up to 350°F (175°C) within a time span of 30 to 60 minutes. At the temperature of 350°F (175°C) a pressure of approximately 40 psi (276 kPa) is applied for 60 minutes.

The bonded specimen is then cooled and removed.

Specimen dimensions (width, length of overlap and adherend thickness) are in accordance with ASTM D1002 specifications. The shear stress in the lap joints is assumed to be uniform and is calculated by dividing the load applied to the adherends by the overlap area. The mechanical testing of the FM 73, FM 300 and Polyimidesulfone-titanium specimens was performed at Clarkson College of Technology by the methods described in the following paragraphs. All test specimens were prepared at NASA-Langley Research Center.

Geometrical Measurements

Precision measurement of bondline thicknesses and bondline lengths were done with the aid of a microscope under a magnification of 40X. Twenty-five or twenty-six measurements of the bondline thickness and one measurement of the bondline length were taken along both sides of the overlap area. The average bondline thicknesses were used in calculating shear strains which were defined as bondline deformation divided by the average bondline thickness. Adherend width and thicknesses were measured with the aid of a Kanon Dial Caliper.

Single lap specimen dimensions (width, length of overlap and bondline thickness) for the FM 73, Thermoplastic Polyimidesulfone, and FM 300-titanium specimens are given in tables two thru four, respectively, in Appendix B. All dimensions listed are in both English and Metric units.

A high precision, air cooled clip-on gage was used for shear strain measurements. Two notches were milled 0.99 inches (2.51 cm) apart on the overlap side of the single lap specimens so that the

clip-on gage could be attached in them (figure 1). The notches were 0.1 inch (0.254 cm) deep and 0.01 inch (0.0254 cm) wide. Stress concentrations due to the notches in the adherends were estimated to be negligible. Any adherend deformation that occurred within the measuring range of the clip-on gage was calculated and subtracted from the experimental data to obtain the adhesive strains. Such adherend deformations were calculated with the use of the equation:

$$\text{Adherend Deformation} = [F(D-O)]/[E(AT)W] \qquad (22)$$

where

F = load applied to the adherends.

D = the distance between the milled notches in the adherends of the single lap specimen, 0.99 inches (2.51 cm)

O = overlap length

E = Young's Modulus for titanium, 15,000,000 psi (103,421 MPa)

AT = adherend thickness, 0.05 in. (0.127 cm)

W = adherend width over the overlap area.

The clip-on gage was calibrated with a high magnification extensometer calibrator. Load and strain charts were obtained from a three channel strip chart recorder. The output signal from the clip-on gage was amplified through the mechanical testing machine's internal amplifier system. All test specimens were stored at approximately 70°F (21°C) temperature and 65 % relative humidity.

Testing Methods

Groups of twenty-four to twenty-eight single lap specimens bonded with the model adhesives were provided by the NASA-Langley Research Center. The mechanical testing of these single lap specimens were

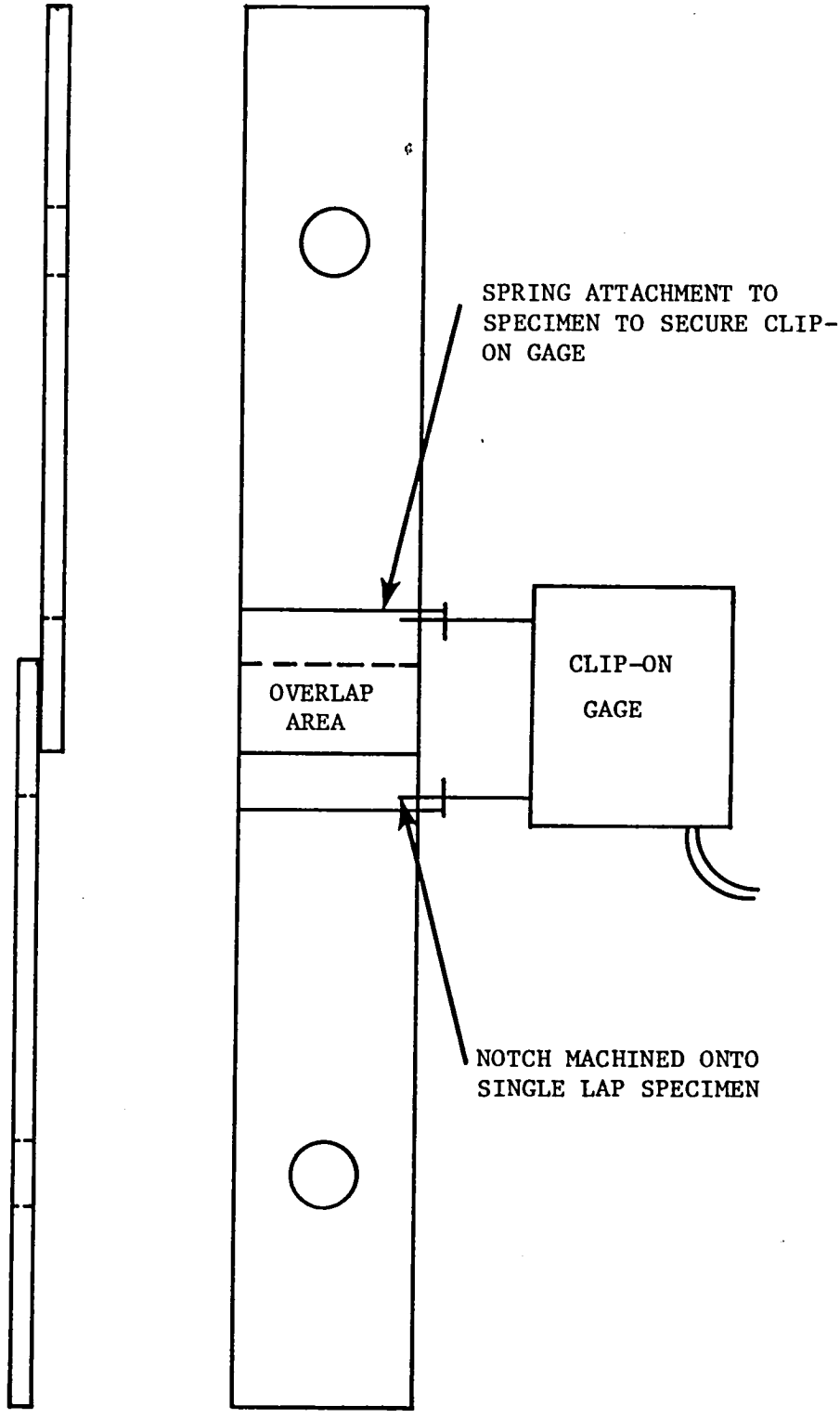

Figure 1. Clip-on Gage Attachment to the Single Lap Specimen for Adhesive Deformation Measurement.

performed either on a Tinius-Olsen Universal testing machine or on a Model 1331 Instron Servohydraulic testing machine depending on their availability.

Room temperature constant strain rate tests were performed at crosshead rates of >0.0, 0.1, 1, 5 and 10 in/min (>0.0, 0.254, 2.54, 12.7 and 25.4 cm/min). High temperature constant strain rate tests were performed at a crosshead rate of 5 in/min (12.7 cm/min). Room and high temperature creep tests were performed with an initial crosshead rate of 0.3 in/min (0.76 cm/min). Each adhesive was tested in creep at least at four different stress levels above the elastic limit shear stress (found from both room and high temperature constant strain rate tests) and at three or four different temperature levels. The FM 73 adhesive creep tests were performed at temperature levels of 70°F (21°C), 130°F (54°C) and 180°F (82°C). The Thermoplastic Polyimidesulfone adhesive creep tests were performed at temperature levels of 70°F (21°C), 250°F (121°C), 350°F (177°C) and 450°F (232 °C). The FM 300 adhesive creep tests were performed at temperature levels of 70°F (21°C), 180°F (82°C), 250°F (121°C) and 300°F (148°C). The maximum test temperature for each adhesive was determined on the basis of product information available in the literature [10,11,12].

The high temperature creep and constant strain rate tests were performed with the aid of an environmental chamber which was attached to the testing machine. Deformation and load signal outputs from the Tinius-Olsen Universal testing machine were recorded on a strip chart recorder and the testing machine's load chart, respectively. Similar outputs from the Instron Servohydraulic testing machine's amplifier were channelled to a PDP-11 Digital computer for processing of the data.

CHAPTER 4

RESULTS AND DISCUSSION

This chapter compares the analytical methods reviewed in Chapter 2 with the experimental constant strain rate, creep and creep-rupture behavior of FM 73, FM 300 and Thermoplastic Polyimidesulfone adhesives. The suitability of the proposed theoretical method for prediction of adhesive material behavior is, therefore, assessed. Results on FM 73 will be discussed first.

Results on FM 73 Adhesive

The constant strain rate shear stress-strain behavior of FM 73 adhesive at two different shear strain rates is shown in figure 2. A region of linear elastic behavior followed by a region of viscoelastic behavior is observed, thereby, suggesting that the modified Bingham model may be used to describe the constant strain rate shear stress-strain behavior of FM 73 adhesive. Comparison of experiment and theory reveals that the modified Bingham model provides a good fit to the experimental data. The constants (namely θ, μ, $\dot{\gamma}$ and G) used in fitting the model to the experimental data are also shown in figure 2.

The elastic shear modulus, G, for FM 73 adhesive was taken to be equal to the initial slope of the constant strain rate shear stress-strain curve (figure 2). The value for G, as given in figure 2, is about ten times less than the value obtained by using the relation

$$G = E/(2 + 2\nu) \tag{23}$$

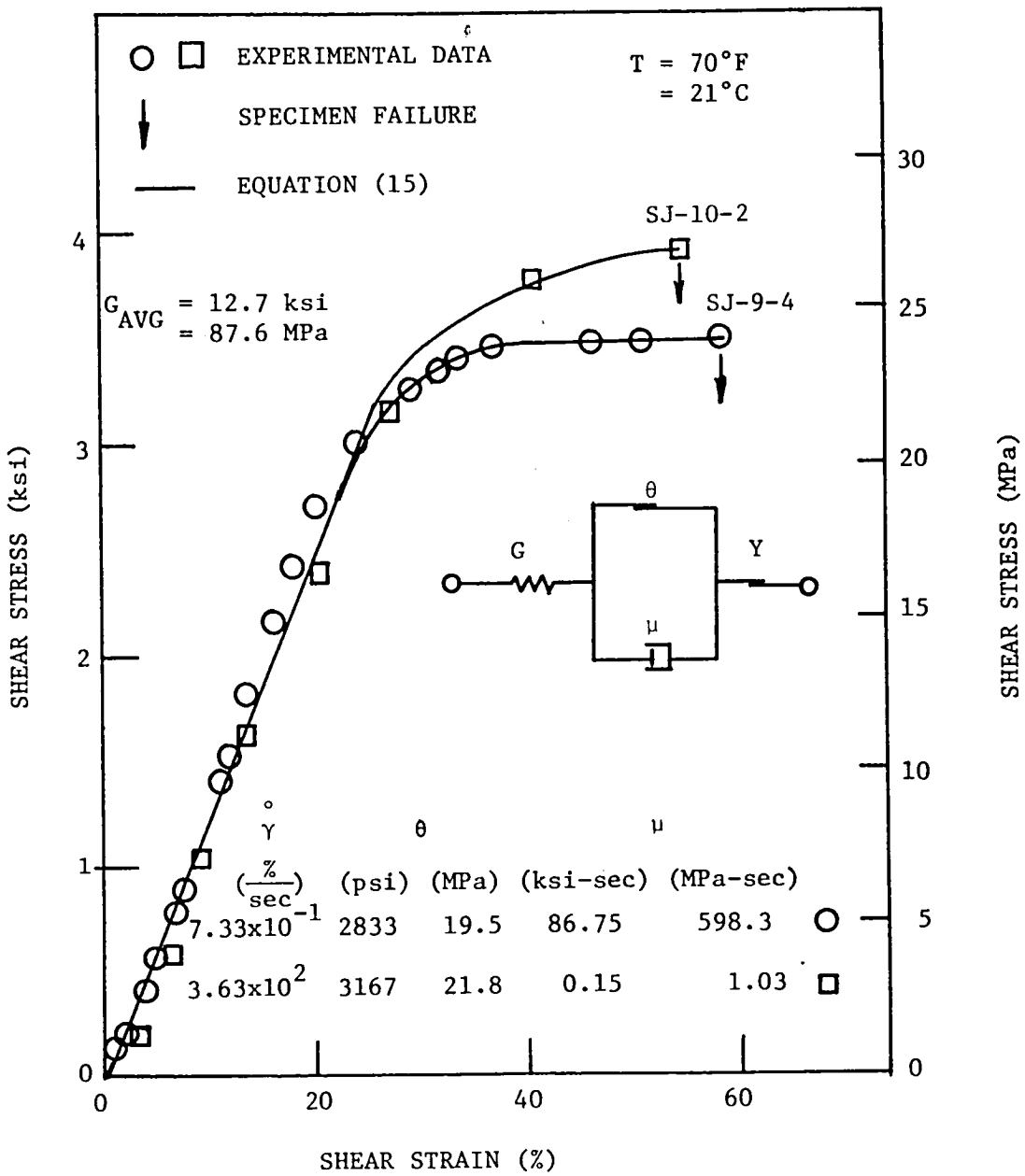

Figure 2. Constant Strain Rate Stress-Strain Behavior of FM 73 and Comparison with Theory.

where

ν = poisson's ratio and,

E = elastic modulus in tension [10, 14]

The authors believe that this difference is caused by:

1) Nonuniform shear stress distribution and the presence of tearing stresses in single lap geometry;

2) The effect of specimen geometry changes, during loading, on adhesive deformation measurement (i.e. bending of the overlap area);

3) Involuntary inclusion of some adherend deformation during adhesive shear deformation measurements;

4) Inappropriate comparison of bulk tensile measurements with bonded (thin layer) shear measurements for adhesives with carrier cloths.

It should be noted that the observed differences between the measured and calculated "G" values is not of major concern for the present study, since the measured values are used only in a comparative manner to assess the effects of rate, time and temperature on the adhesive behavior. Furthermore, the authors believe that the measured mechanical behavior should have practical value as it represents the actual in-service behavior of a very common joint geometry.

Results from the constant strain rate tests for FM 73 adhesive (figure 2) revealed that the ultimate shear stresses are rate dependent. This rate dependent variation in the ultimate shear stresses with the initial elastic shear strain rate is shown in figure 3. A 12% increase in the joint strength over a 500 times increase in the

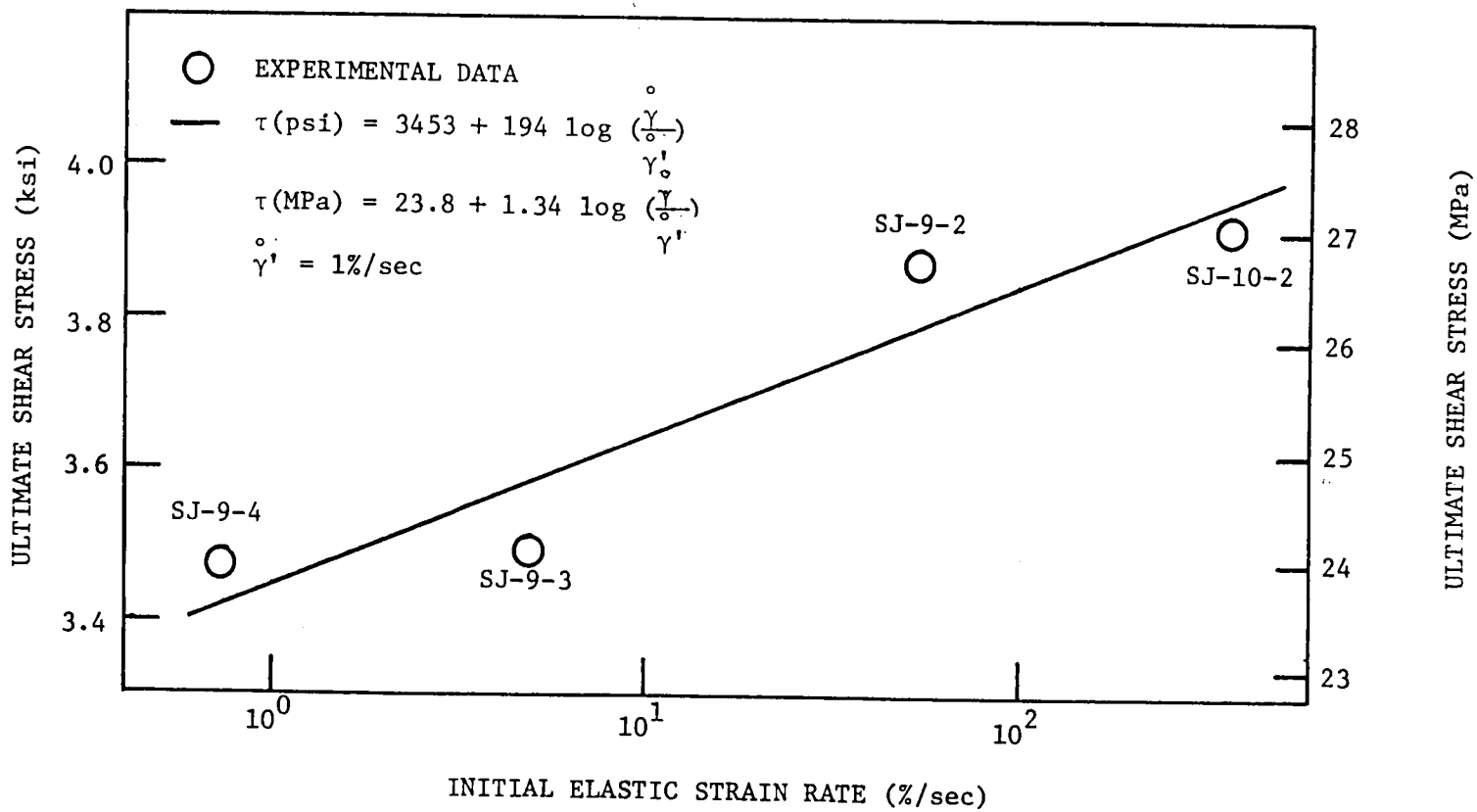

Figure 3. Variation of Ultimate Shear Stress with Initial Elastic Strain Rate and Comparison with Ludwik's Equation for FM 73 Adhesive.

shear strain rate is observed. Figure 3 also reveals that Ludwik's equation (equation 1) provides a good fit to the experimental data.

Figure 4 shows variation of maximum shear strain with initial elastic shear strain rate. Experimental data indicates a decrease in the maximum shear strain values with an increase in the shear strain rate as would be expected for materials that exhibit viscoelastic behavior. An empirical equation representing the data is also shown in figure 4.

Variation of elastic limit shear stress with initial elastic shear strain rate is shown in figure 5. Apparently, Ludwik's equation provides a good fit to the experimental data.

The constant strain rate shear stress-strain behavior of FM 73 adhesive at elevated temperatures is shown in figure 6. As expected, the ultimate shear stress decreases with an increase in the environmental temperature. In comparison to the room temperature condition, the ultimate shear stress is $\sim 31\%$, 53% and 87% lower at $130^{\circ}F$ ($54^{\circ}C$), $180^{\circ}F$ ($82^{\circ}C$) and $250^{\circ}F$ ($121^{\circ}C$) conditions, respectively. It can also be observed that the maximum shear strains increase at elevated temperatures.

Room temperature creep behavior of FM 73 adhesive is shown in figure 7. As may be seen, significant viscoelastic-plastic effects (in the tertiary region) are evident at the higher stress levels.

The creep response of FM 73 at $130^{\circ}F$ ($54^{\circ}C$) and $180^{\circ}F$ ($82^{\circ}C$) conditions is shown in figures 8 and 9, respectively. Higher magnitudes of shear strains are reached at elevated temperatures, especially at lower stress levels. The sudden plastic flow to failure (The tertiary region) observed at room temperature (figure 7) is not

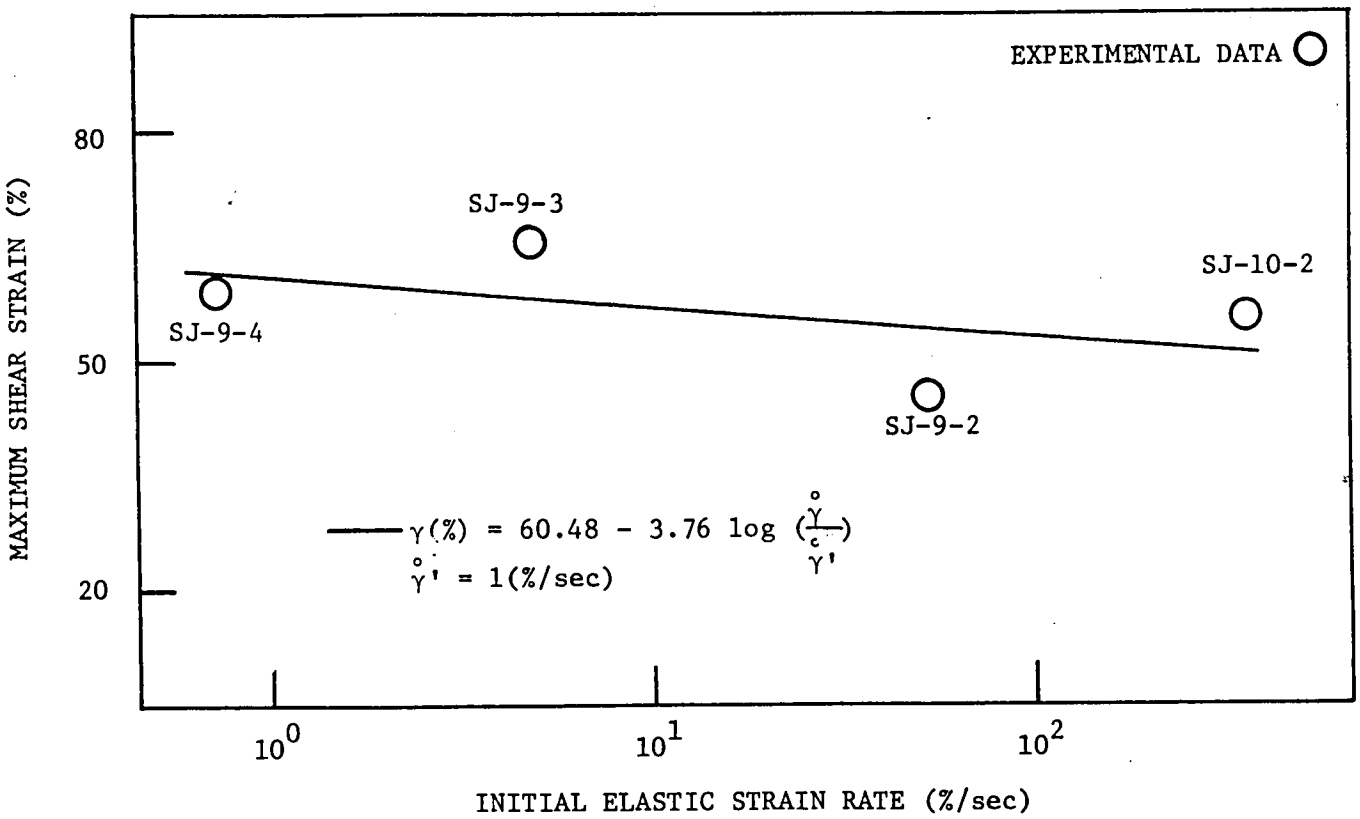

Figure 4. Variation of Maximum Shear Strain with Initial Elastic Strain Rate for FM 73 Adhesive.

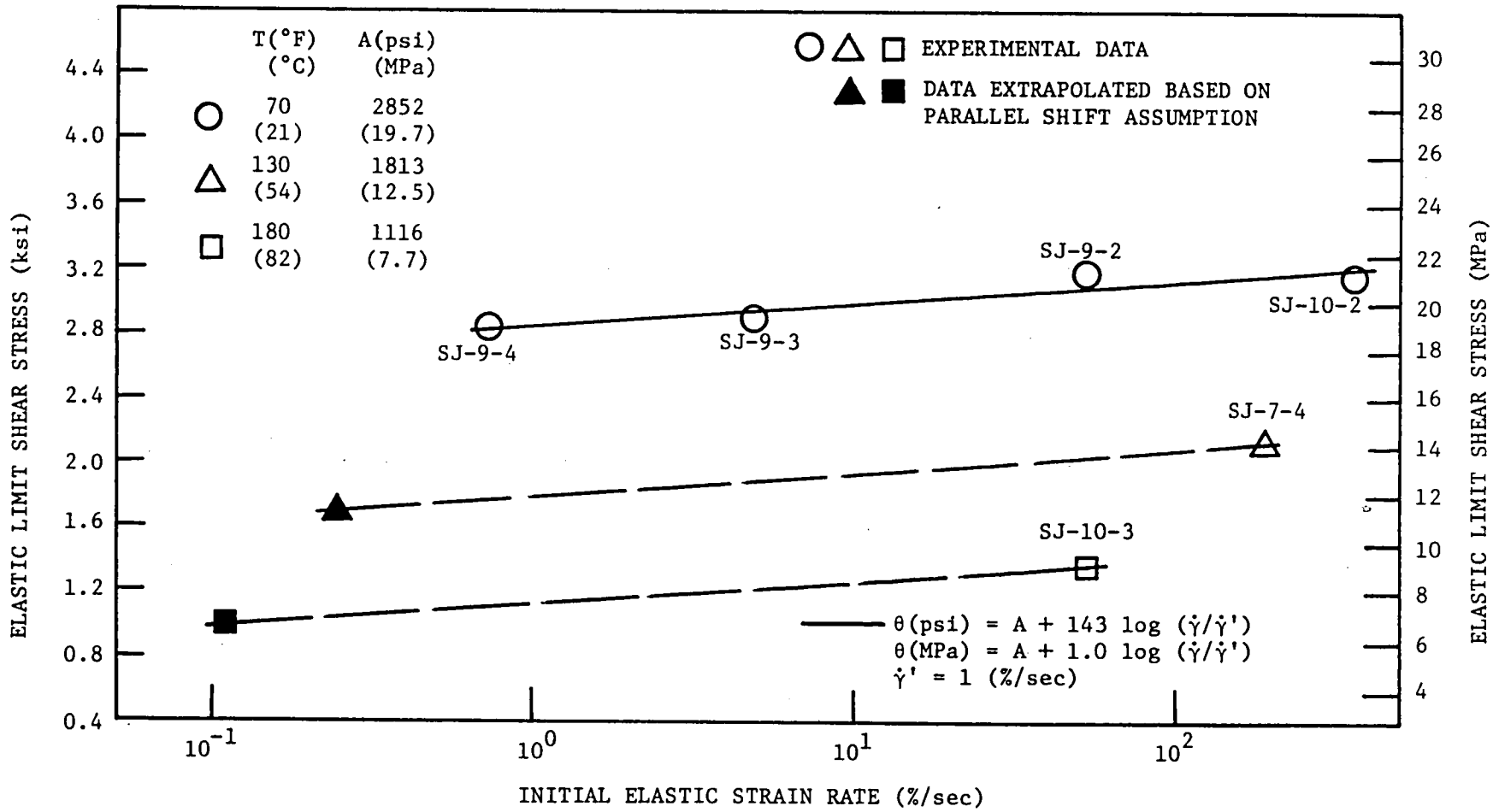

Figure 5. Variation of Elastic Limit Shear Stress with Initial Elastic Strain Rate and Comparison with Ludwik's Equation for FM 73 Adhesive.

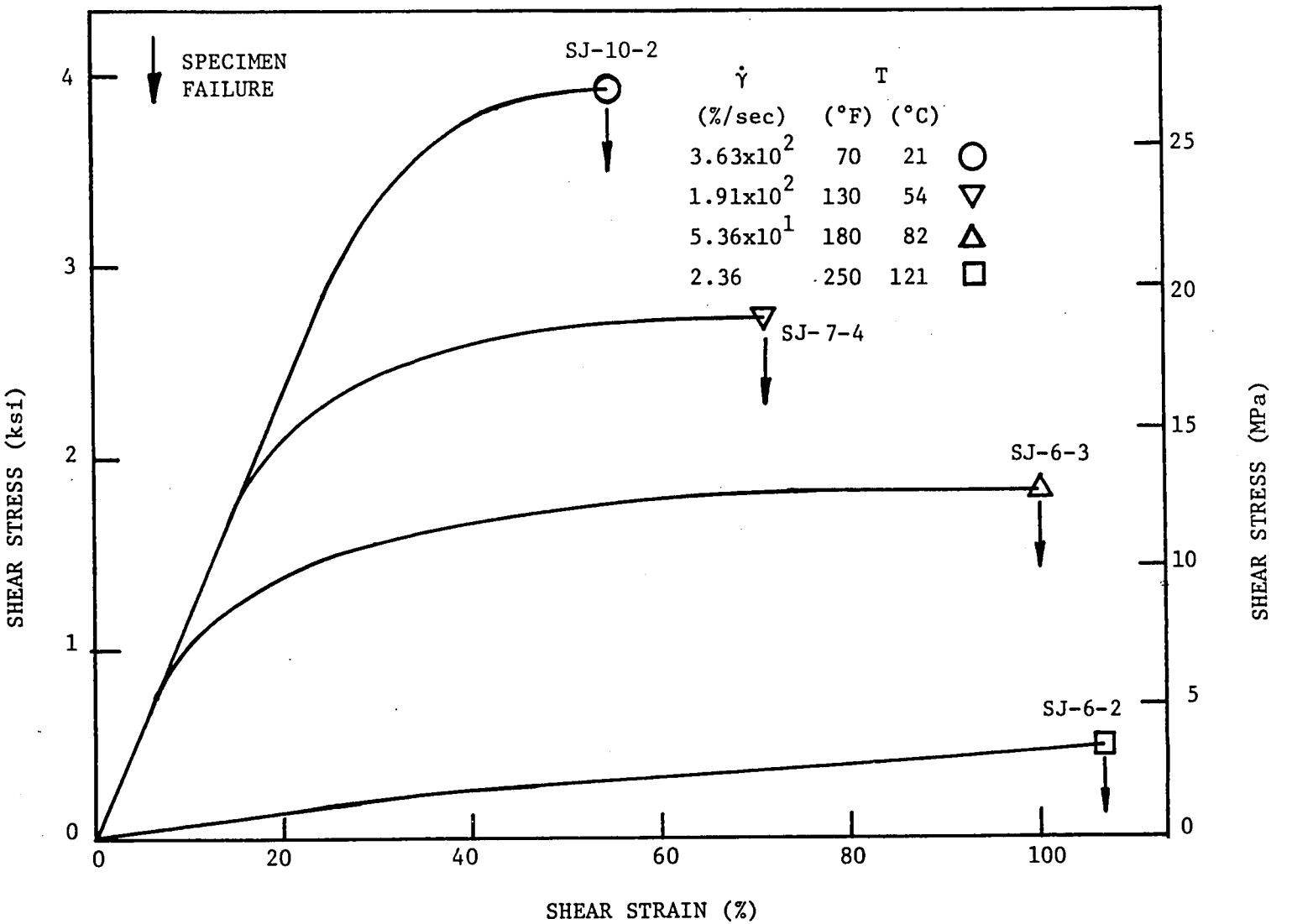

Figure 6. The Effects of Temperature on the Constant Strain Rate Stress-Strain Behavior of FM 73 Adhesive.

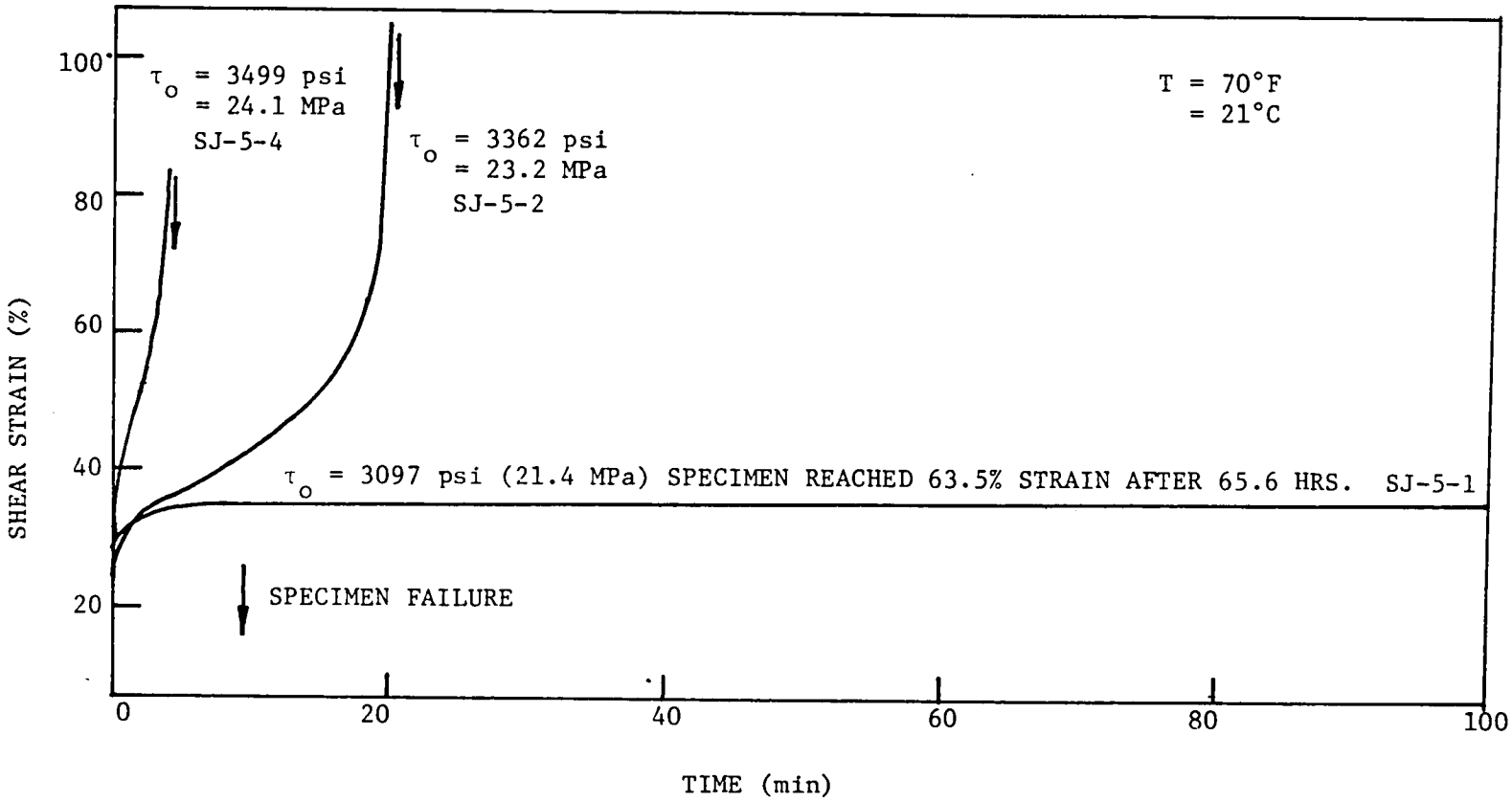

Figure 7. Room Temperature Creep Response of FM 73 Adhesive.

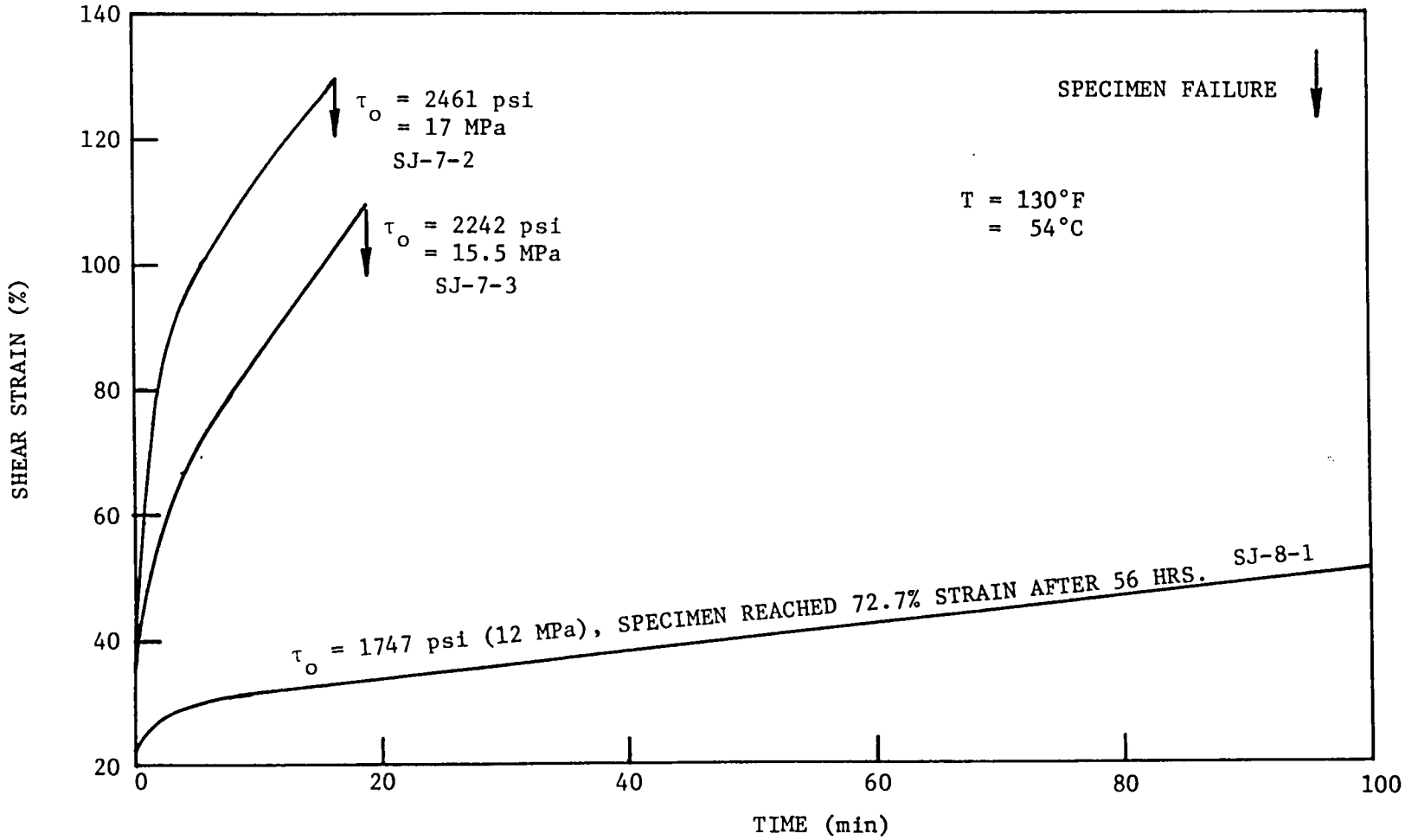

Figure 8. Creep Behavior of FM 73 Adhesive at 130°F (54°C) Condition.

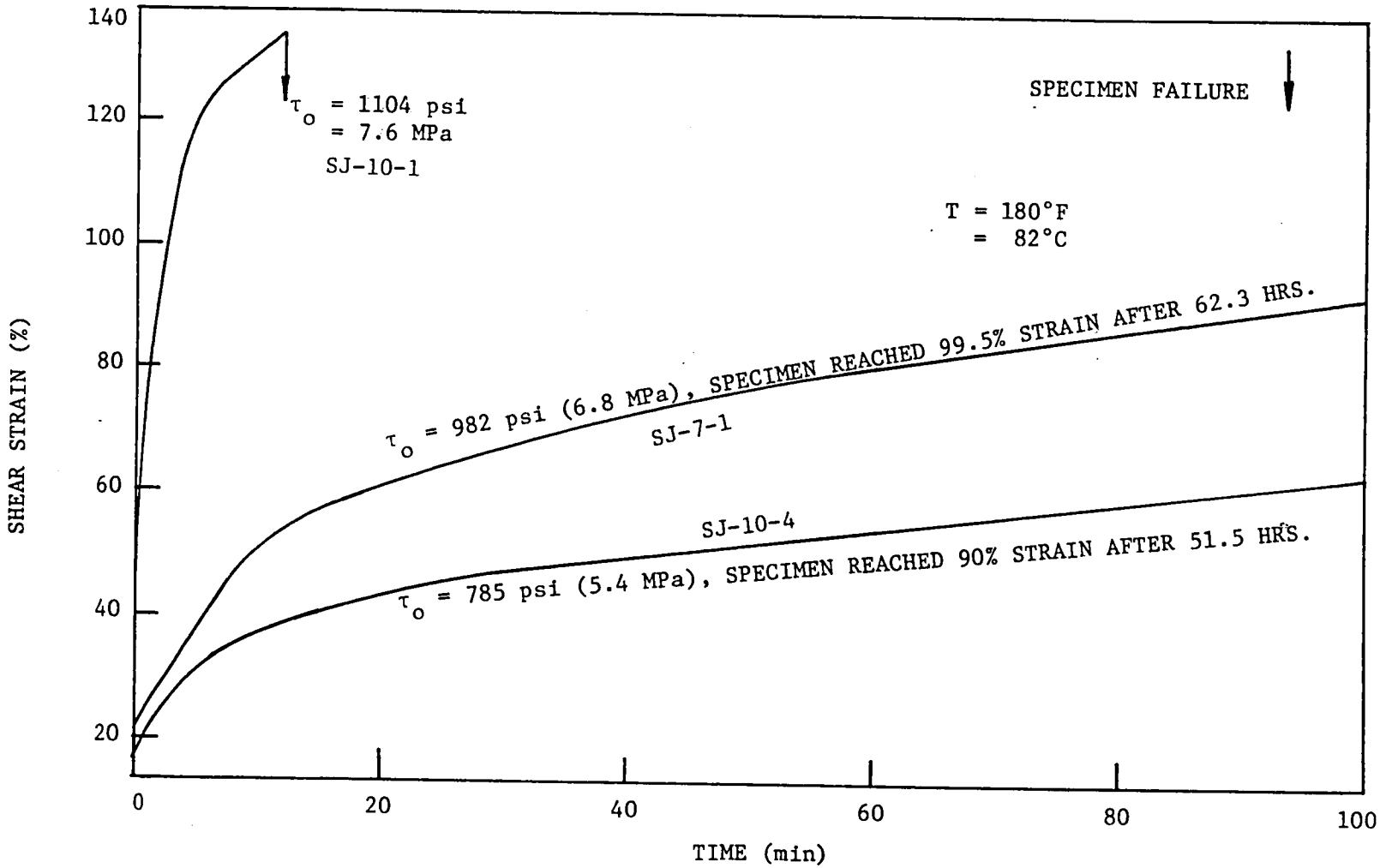

Figure 9. Creep Behavior of FM 73 Adhesive at 180°F (82°C) Condition.

evident at elevated temperatures.

Creep-rupture data for FM 73 is shown in figures 10 and 11. Figure 10 illustrates the comparison of Zhurkov's (modified) equation (equation 7) with the experimental data. As may be observed, data and theory show good agreement at elevated temperatures. The room temperature data, however, does not show agreement with theory. The constants U_o and γ used to fit Zhurkov's equation to the creep-rupture data are also shown in figure 10.

Comparison of the creep-rupture data with Crochet's equation (equation 8) is shown in figure 11. It can be seen that the behavior is a decaying exponential one with respect to time. The plots reach an asymptotic stress level, below which creep failures are not expected to occur. The highest points in figure 11 (shown as solid black figures) represent ultimate shear stress values obtained from the highest rate shear stress-strain curves.

Figure 11 reveals that the delayed failure behavior of FM 73 can be predicted accurately by employing either the Maxwell or modified Bingham models. The solid and broken lines in figure 11 represent Crochet's relations (equations 20 and 10) based on the modified Bingham and Maxwell models, respectively. The elastic limit stresses, (θ), in equation 20 are determined by extrapolation. Since only one "θ" value corresponding to high rate testing is available at each elevated temperature (figure 6).

The strain rates corresponding to the initial (monotonic) loading portion of the elevated temperature creep tests are lower than those used for instant rupture conditions of figure 11. Such low initial strain rates are applied in the creep testing of bonded specimens to

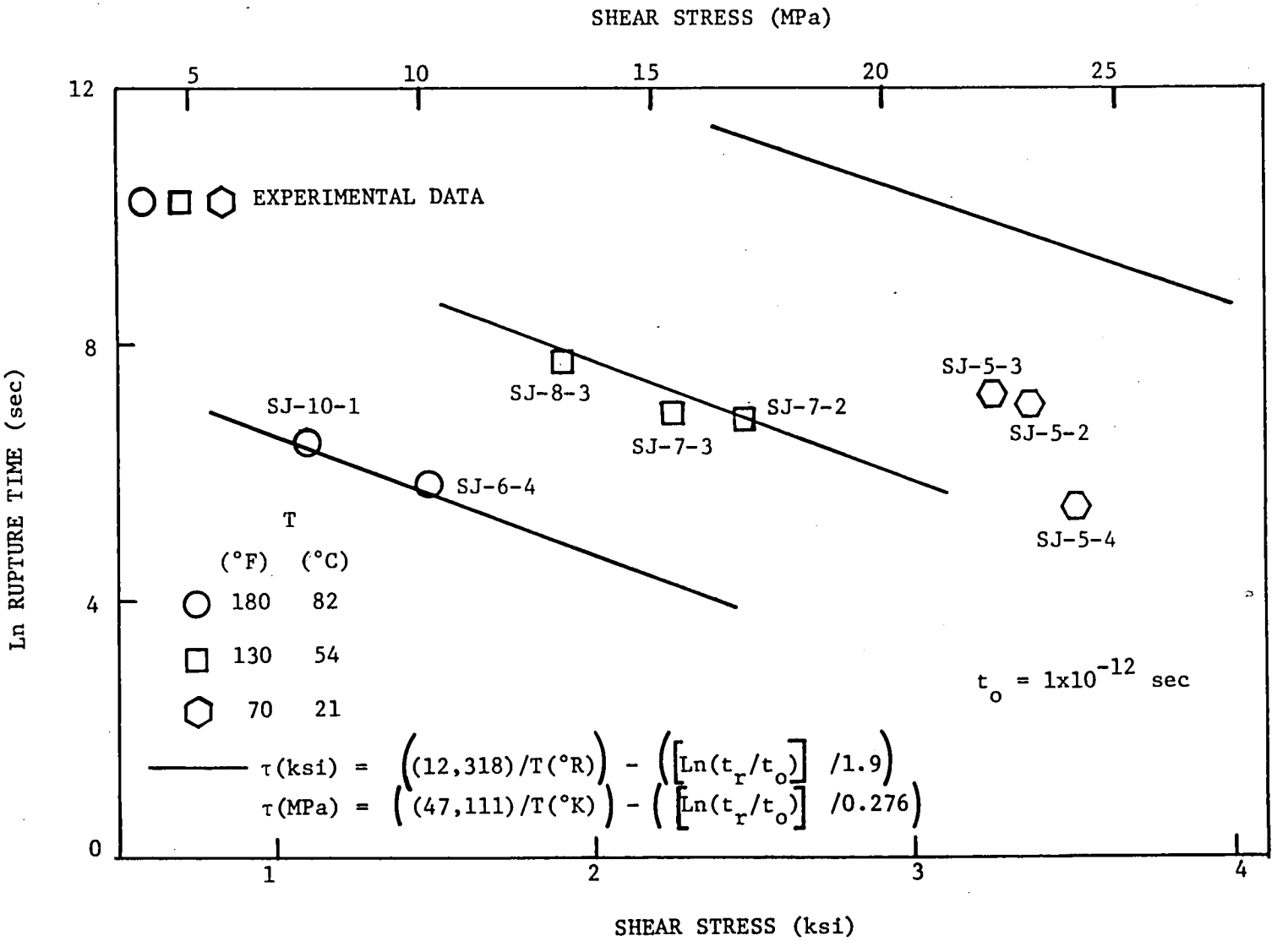

Figure 10. Creep Rupture Data and Comparison with Zhurkov's Equation for FM73 Adhesive.

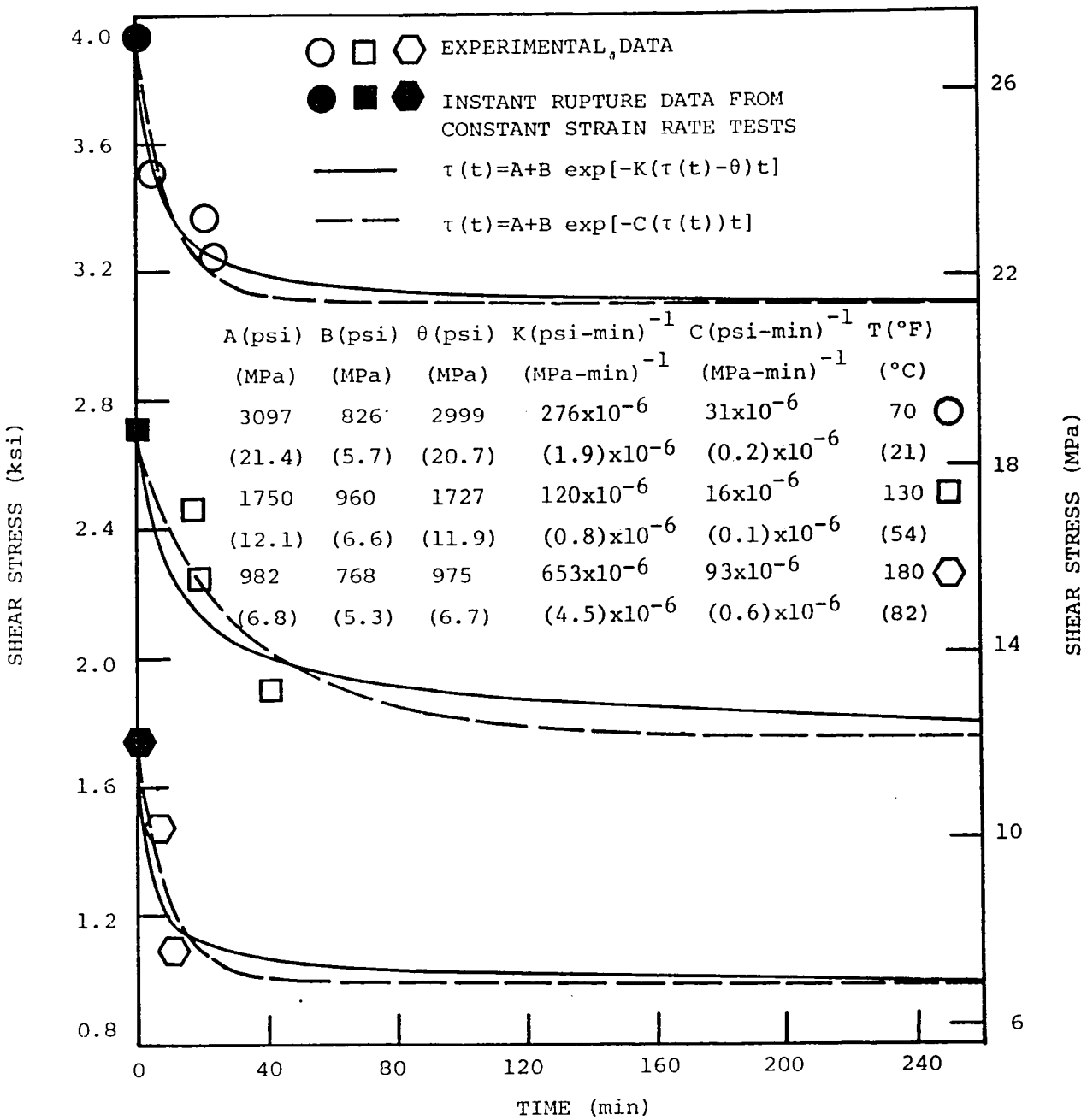

Figure 11. Creep Rupture Data and Comparison with Crochet's Equation for FM 73 Adhesive.

avoid a load overshoot. Consequently, due to the limitation in the number of specimens available, an extrapolation procedure is applied by assuming parallel shifts of Ludwik's equation at elevated temperatures (figure 5) in order to obtain the necessary "θ" values.

Figure 12 shows the variation of the maximum -or safe- level of creep stress values (below which creep failures are not expected to occur) with environmental temperature. The maximum creep stress values represent the asymptotic stress levels (i.e. material constants A in figure 11) obtained with the application of Crochet's equation. Apparently, the relation between the asymptotic shear stress level and temperature is a linear one for the range of data shown.

Results on FM 300 Adhesive

All experimental data presented so far has been for FM 73. Similar tests were conducted for FM 300 and similar results were obtained. The constant strain rate shear stress-strain behavior of FM 300 adhesive at four different shear strain rates is shown in figure 13. The presence of linear elastic behavior followed by a region of viscoelastic behavior which is terminated by plastic flow (especially at the lower strain rate) suggests that the modified Bingham model can be used to describe the constant strain rate shear stress-strain behavior of FM 300 adhesive. Comparison of theory (modified Bingham model) and experiment shows good agreement (figure 13). The constants used in fitting the modified Bingham model to the experimental data are also shown in figure 13.

The variation of the ultimate shear stress with initial elastic shear strain rate for FM 300 adhesive is shown in figure 14.

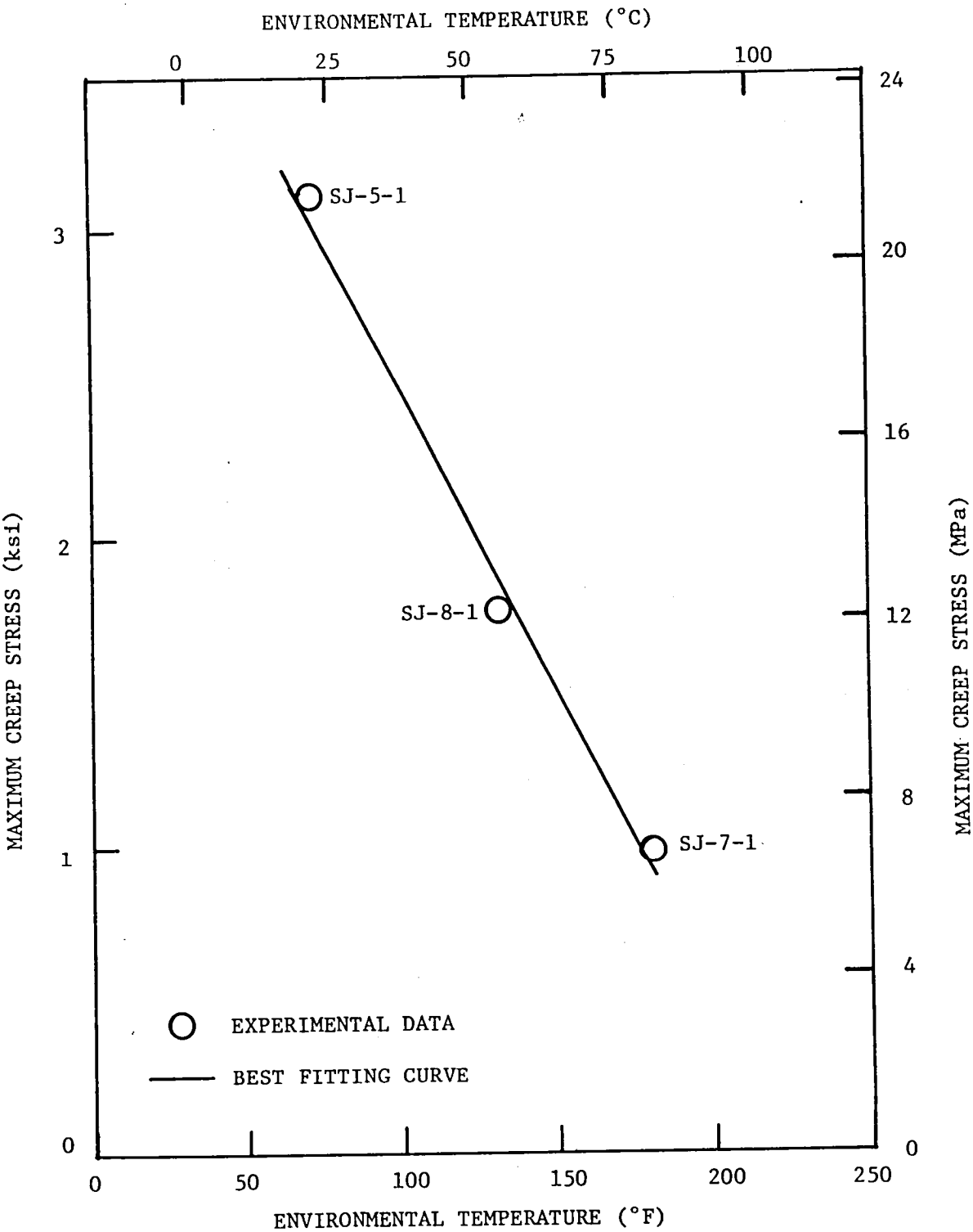

Figure 12. Variation of Maximum (safe) Creep Stress with Environmental Temperature for FM 73 Adhesive.

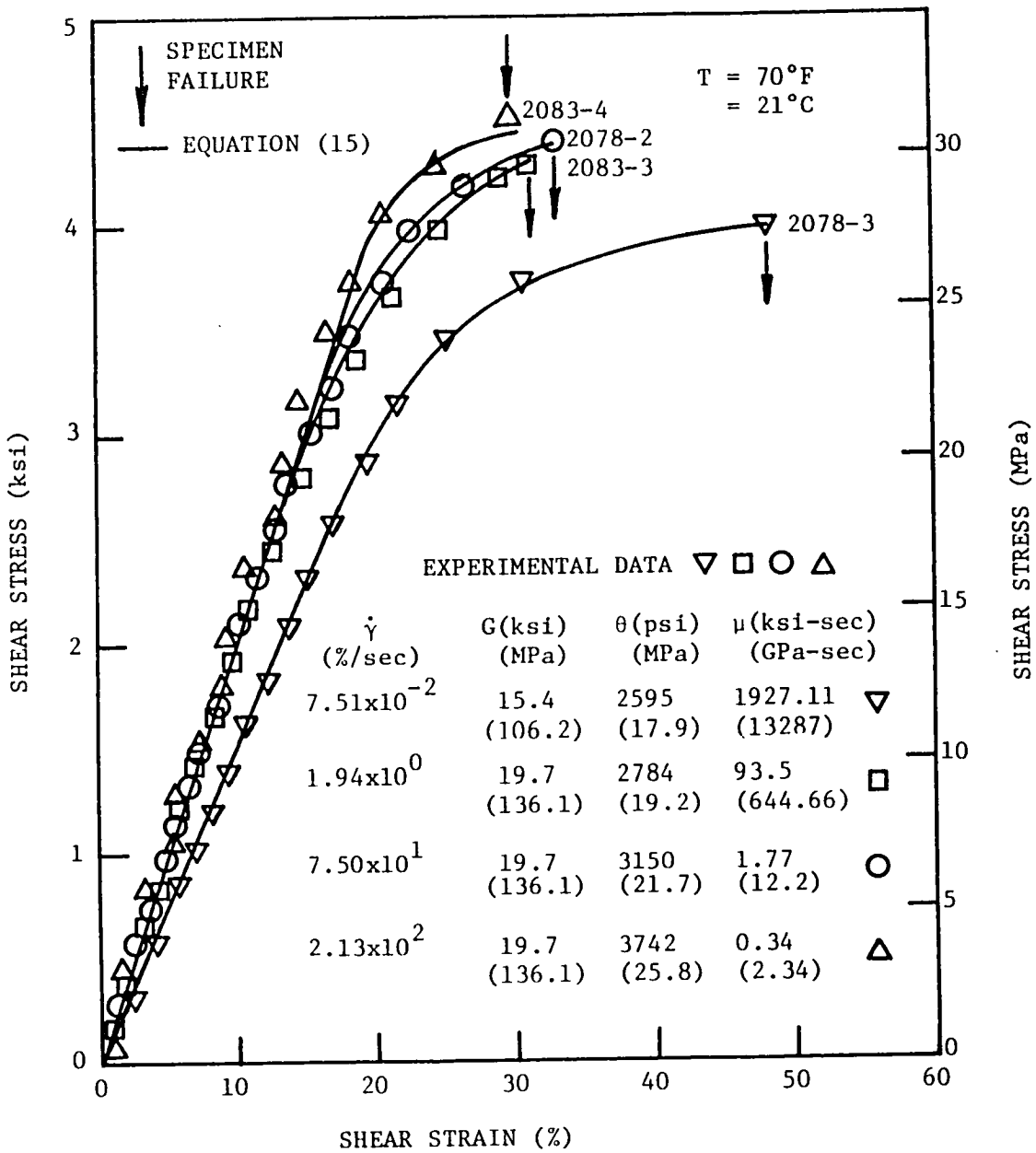

Figure 13. Constant Strain Rate Stress-Strain Behavior of FM 300 and Comparison with Theory.

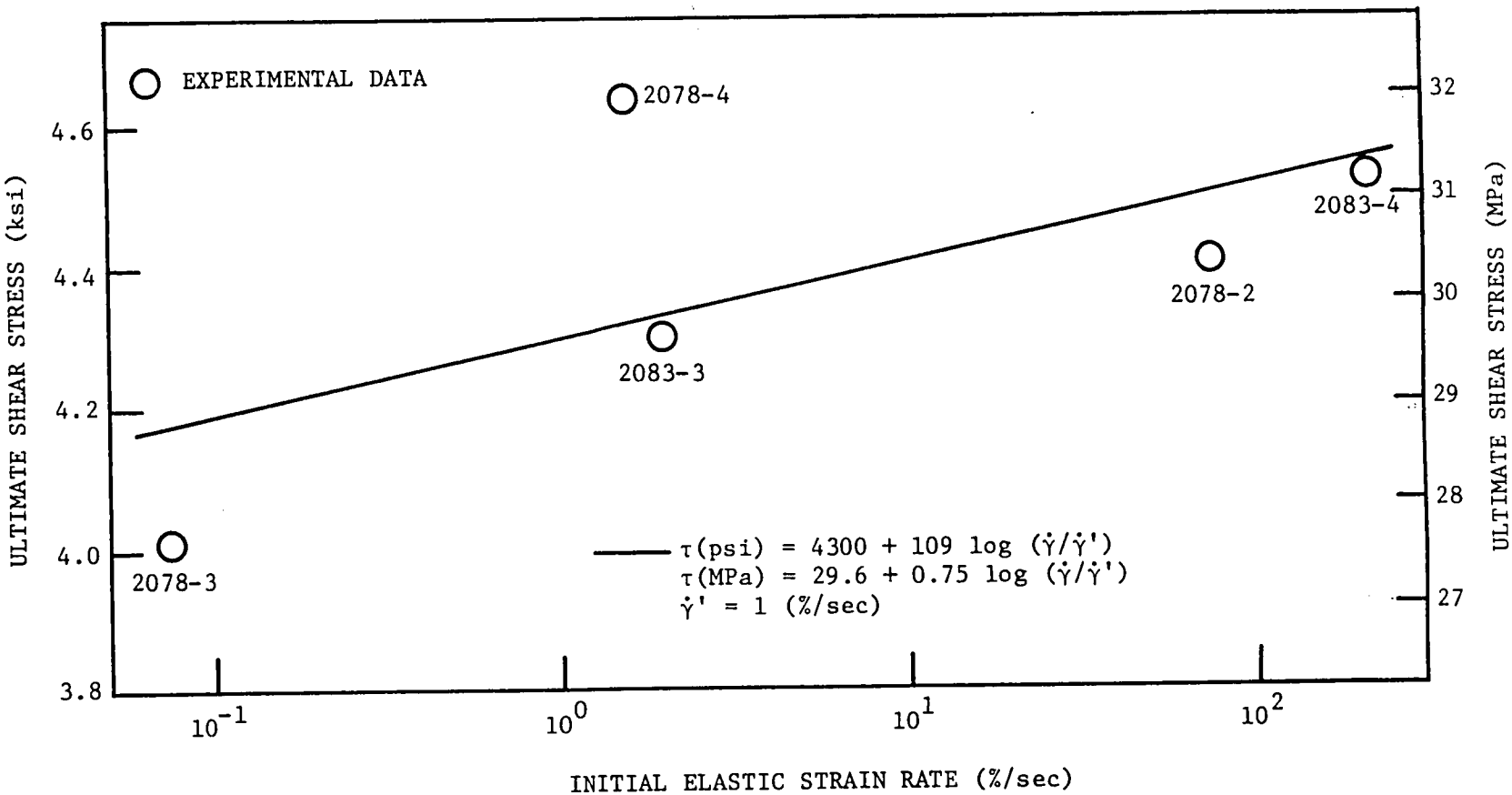

Figure 14. Variation of Ultimate Shear Stress with Initial Elastic Strain Rate and Comparison with Ludwik's Equation for FM 300 Adhesive.

Apparently, a 2800 times increase in the shear strain rate (from 0.0751 to 213 %/sec) results in ~ 13 % increase in the ultimate shear stress. Figure 14 also reveals that Ludwik's equation (equation 1) provides a good fit to the experimental data.

Figure 15 shows variation of maximum shear strain with the initial elastic shear strain rate. Less scatter is observed with the maximum shear strain values in comparison to the maximum shear stress values. The data also indicates a decrease in the maximum shear strain values with an increase in the shear strain rate as would be expected for materials that exhibit viscoelastic behavior. An empirical equation representing the data is also shown in figure 15.

Variation of elastic limit shear stress with initial elastic shear strain rate is shown in figure 16. Apparently, Ludwik's equation provides a good fit to the experimental data.

The effects of temperature on the constant strain rate shear stress-strain behavior of FM 300 is shown in figure 17. In comparison to the room temperature condition, the ultimate shear stress is ~0.5 %, 17 %, and 34 % lower at 180°F (82°C), 250°F (121°C) and 300°F (149°C) conditions, respectively. It can also be observed that, with the exception of the 300°F (149°C) condition, the maximum shear strains increase at elevated temperatures.

Figure 18 shows the room temperature creep behavior of FM 300 adhesive. The sudden plastic flow to failure observed in the room temperature creep behavior of FM 73 adhesive is not present in figure 18. Creep responses of FM 300 at 180°F (82°C), 250°F (121°C), and 300°F (149°C) conditions are shown in figures 19, 20 and 21, respectively. In comparison to the room temperature behavior, higher

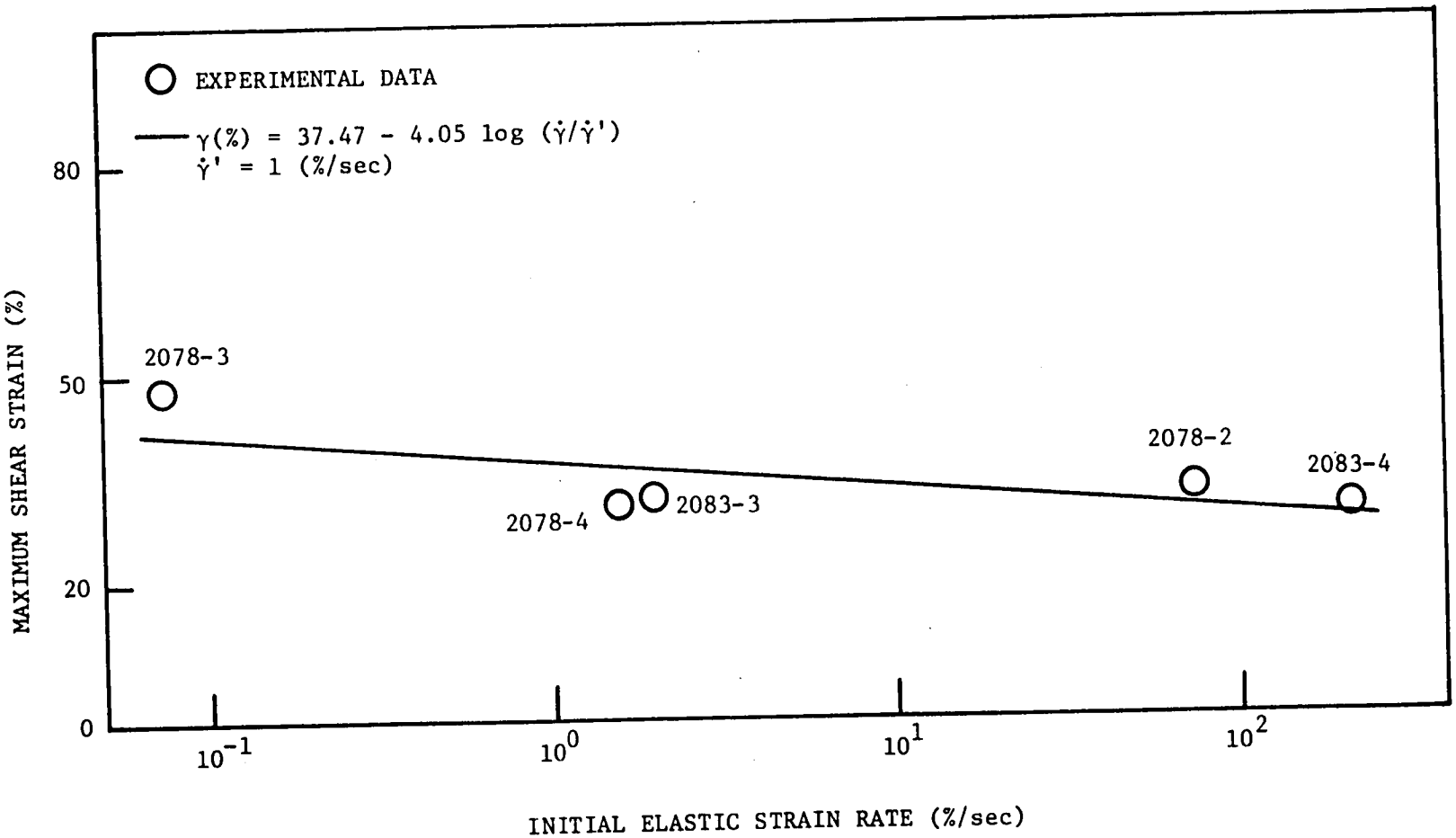

Figure 15. Variation of Maximum Shear Strain with Initial Elastic Strain Rate for FM 300 Adhesive.

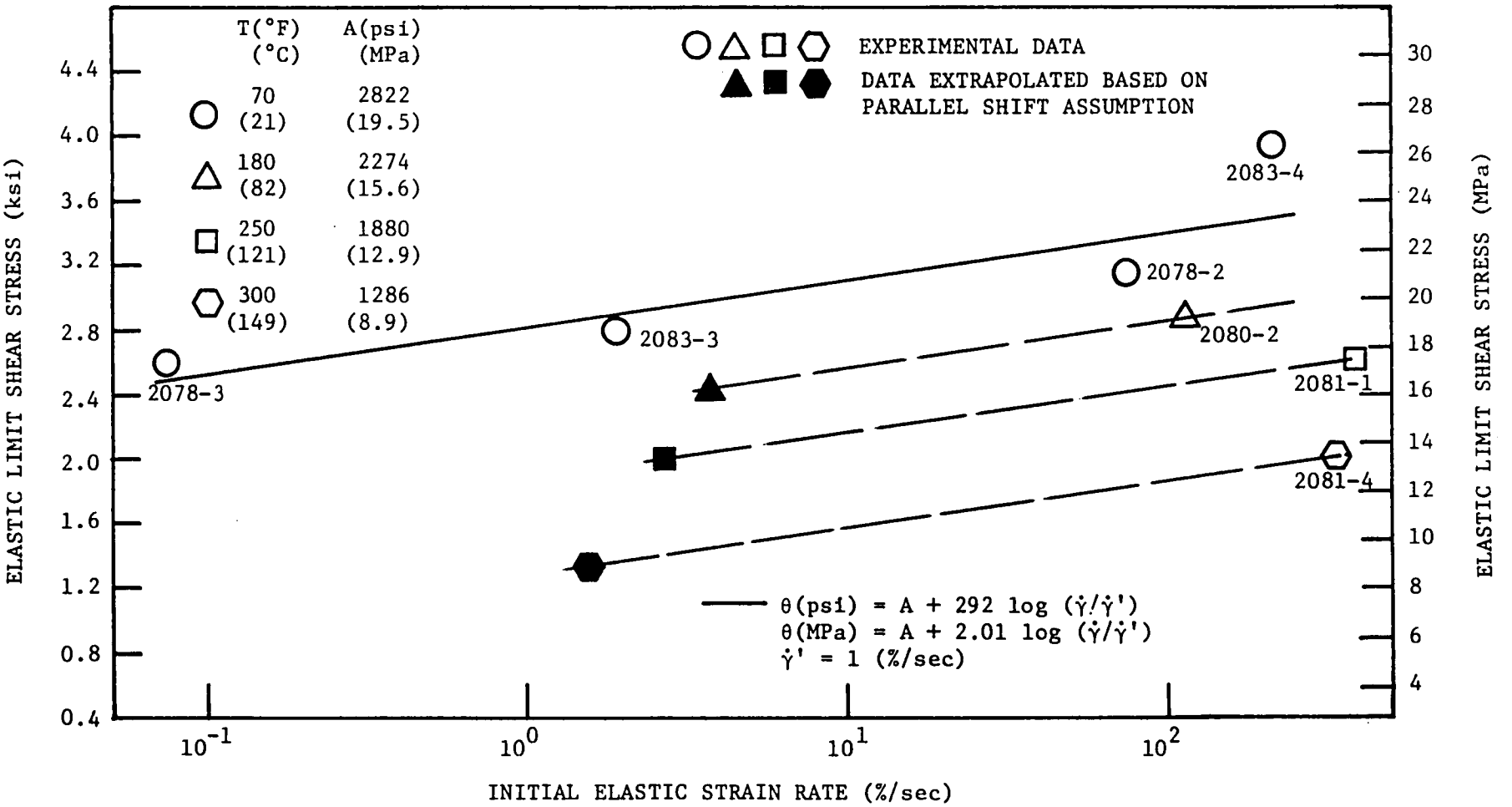

Figure 16. Variation of Elastic Limit Shear Stress with Initial Elastic Strain Rate and Comparison with Ludwik's Equation for FM 300 Adhesive.

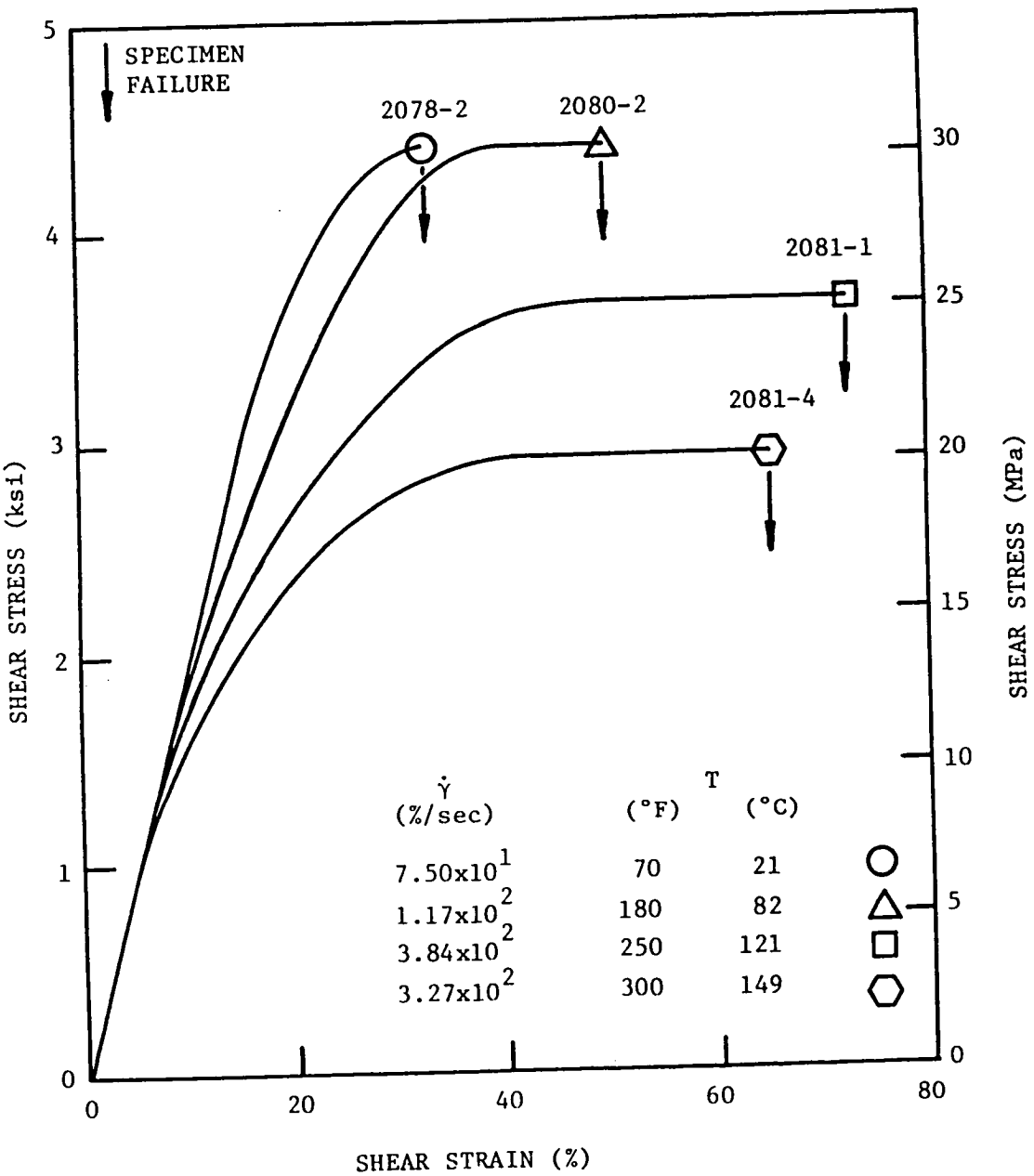

Figure 17. The Effects of Temperature on the Constant Strain Rate Stress-Strain Behavior of FM 300 Adhesive.

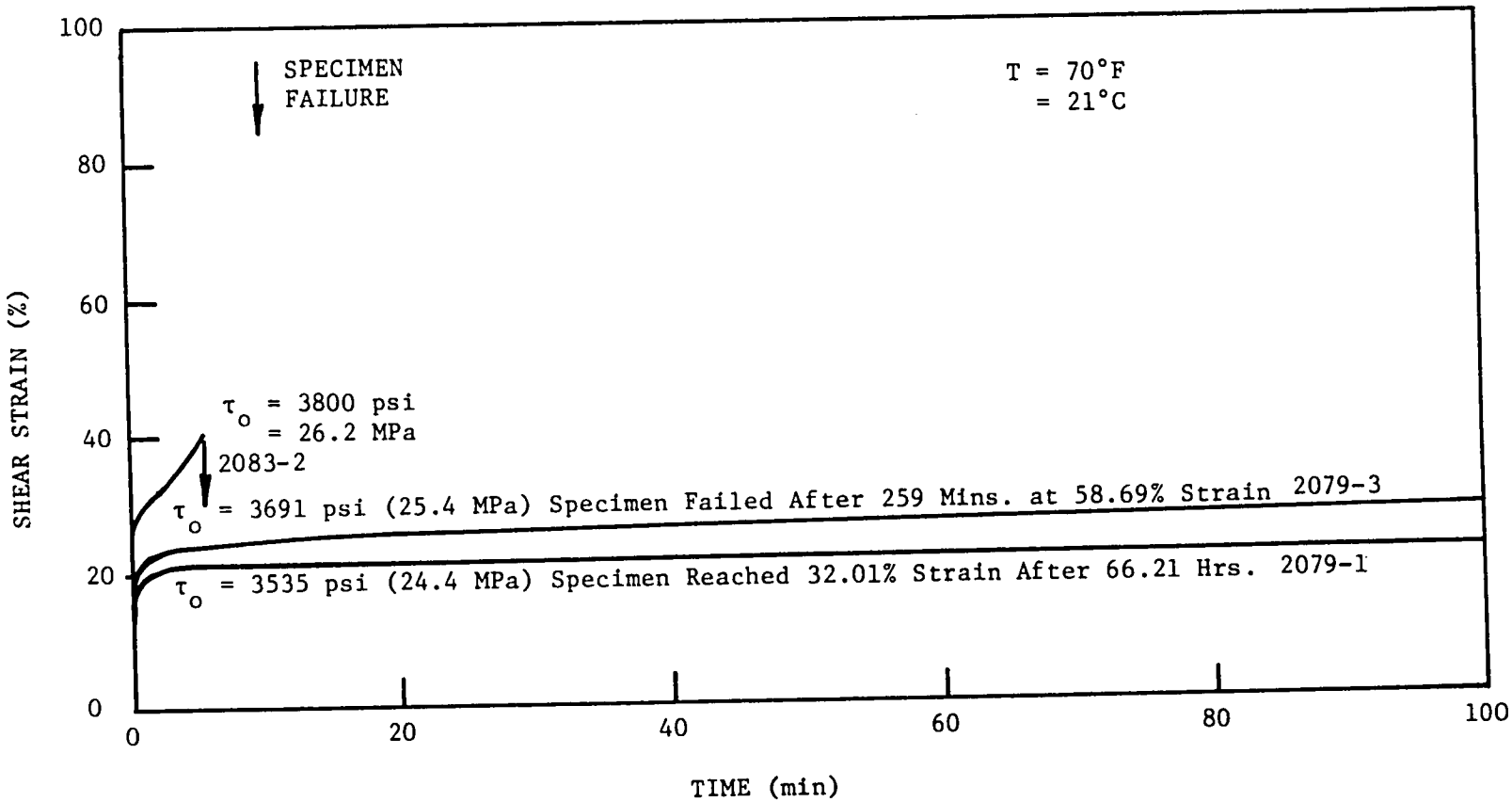

Figure 18. Room Temperature Creep Response of FM 300 Adhesive.

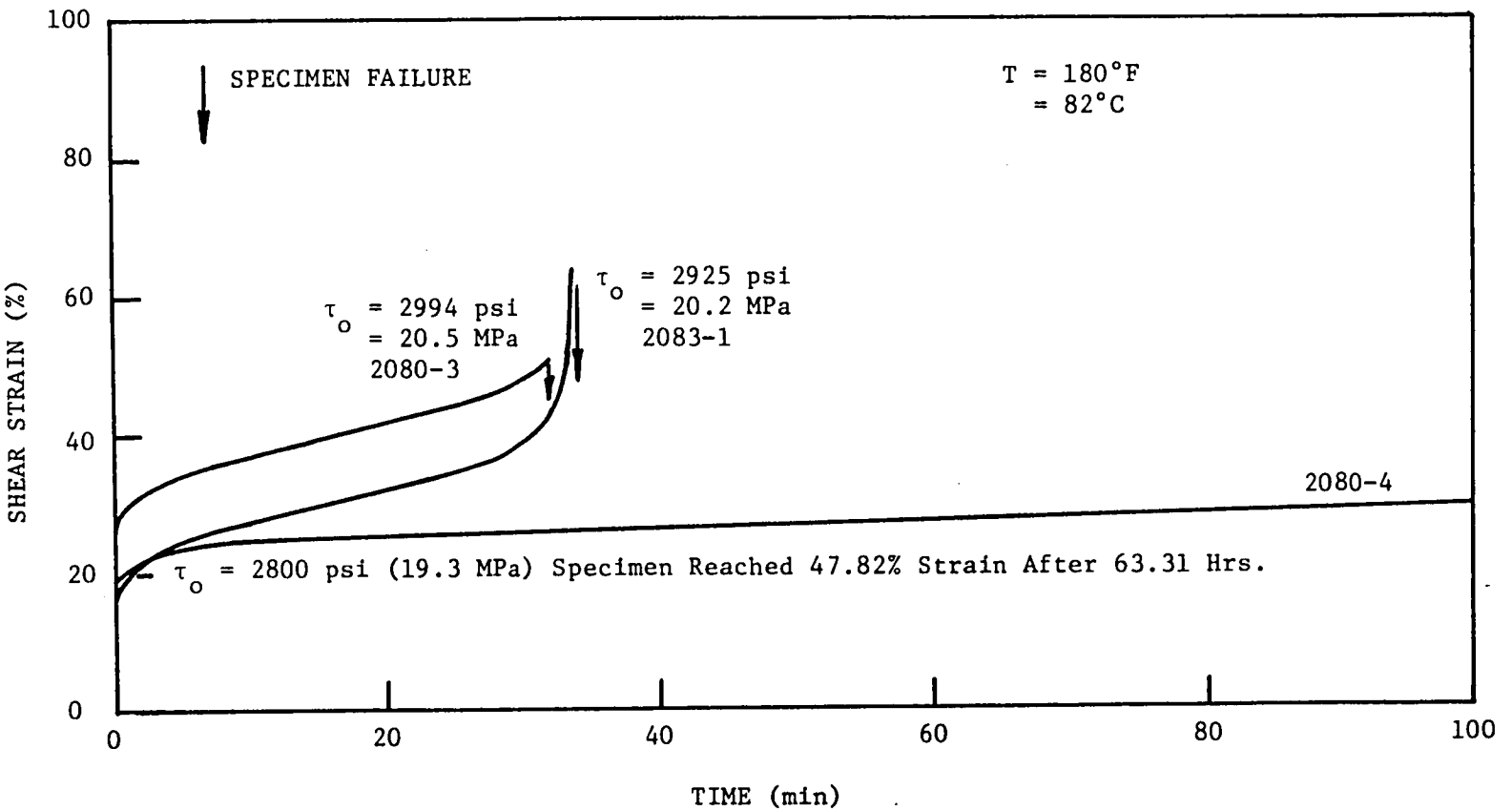

Figure 19. Creep Behavior of FM 300 Adhesive at 180°F (82°C) Condition.

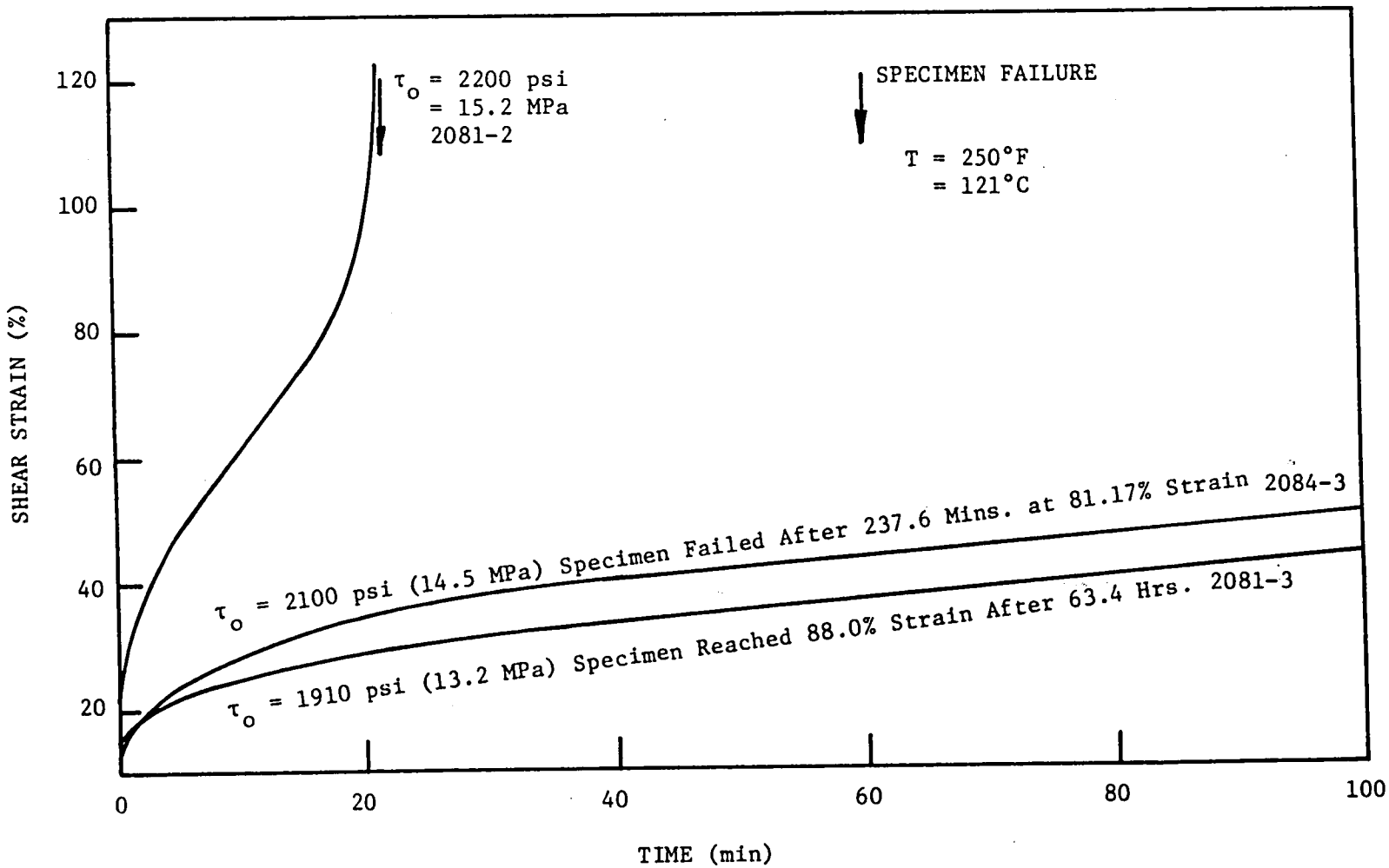

Figure 20. Creep Behavior of FM 300 Adhesive at 250°F (121°C) Condition.

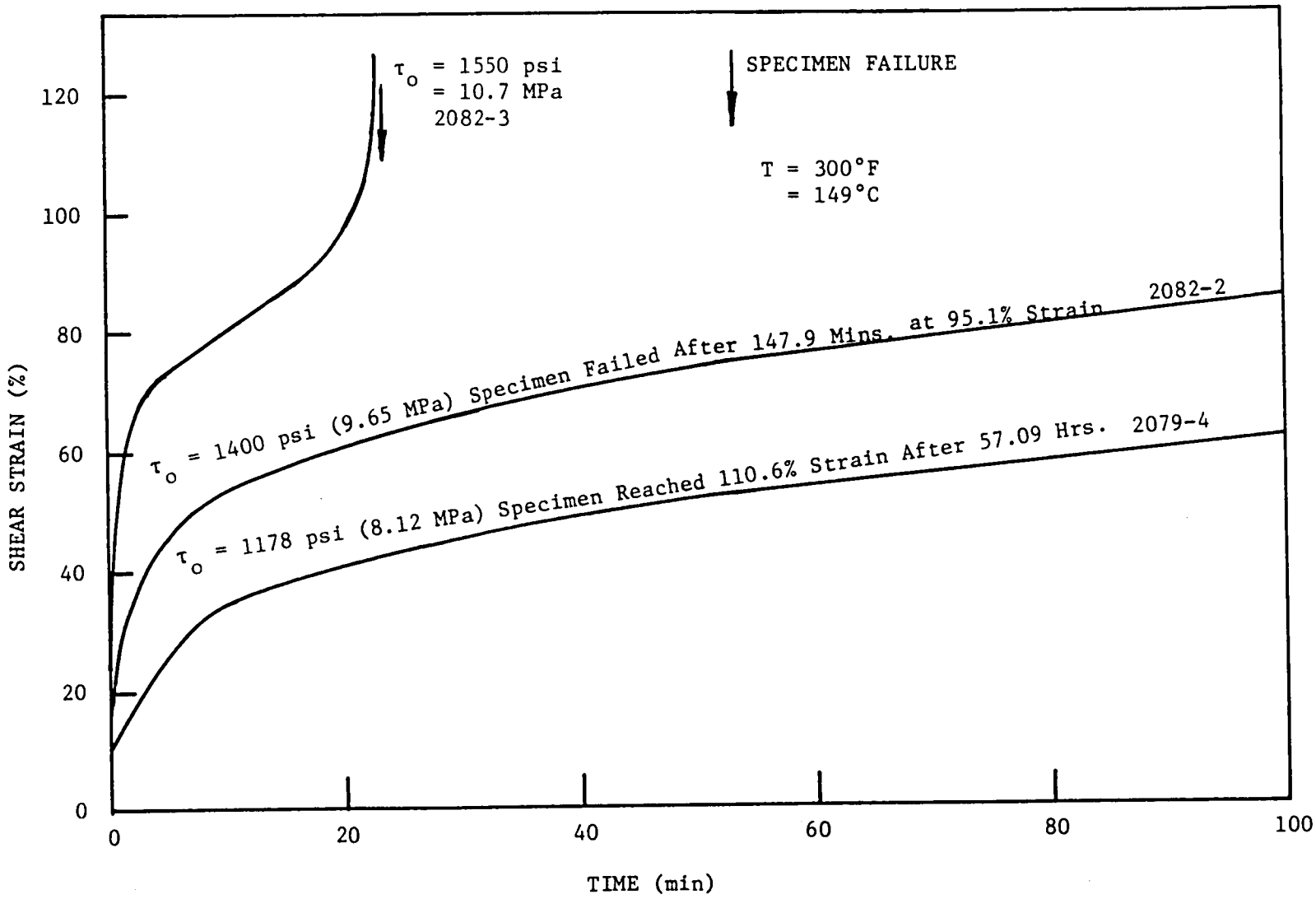

Figure 21. Creep Behavior of FM 300 Adhesive at 300°F (149°C) Condition.

levels of shear strains are reached at comparatively lower levels of shear stresses. Sudden plastic flow to failure (which was not observed with room temperature creep) is evident at elevated temperatures.

Figure 22 shows the comparison of experimental creep-rupture data with Zhurkov's relation (equation 7). Data and theory show poor agreement. Comparison of the creep-rupture data with Crochet's equation based on the modified Bingham and Maxwell models (equations 20 and 10) is shown in figure 23 along with the appropriate constants used to fit the data. The use of the modified Bingham model results in a slightly better fit. It should be noted that the elastic limit stress (θ) values which appear in equation (20) are extrapolated as explained previously for FM 73 adhesive (page 32). The extrapolated data is shown in figure 16.

The authors believe that Crochet's equation provides a better fit to the experimental creep-rupture data in comparison to Zhurkov's equation. Figure 24 shows variation of the maximum - or safe - level of creep stress values (i.e. material constants A in figure 23) with environmental temperature. Apparently, the relation between the asymptotic stress level and temperature is a non-linear one, for the range shown.

Results on Thermoplastic Polyimidesulfone Adhesive

The constant strain rate shear stress-strain behavior of Thermoplastic Polyimidesulfone at two different strain rates is shown in figure 25. The observed weak rate and time dependent behavior suggests that a (non-linear) elastic model may be used to describe the

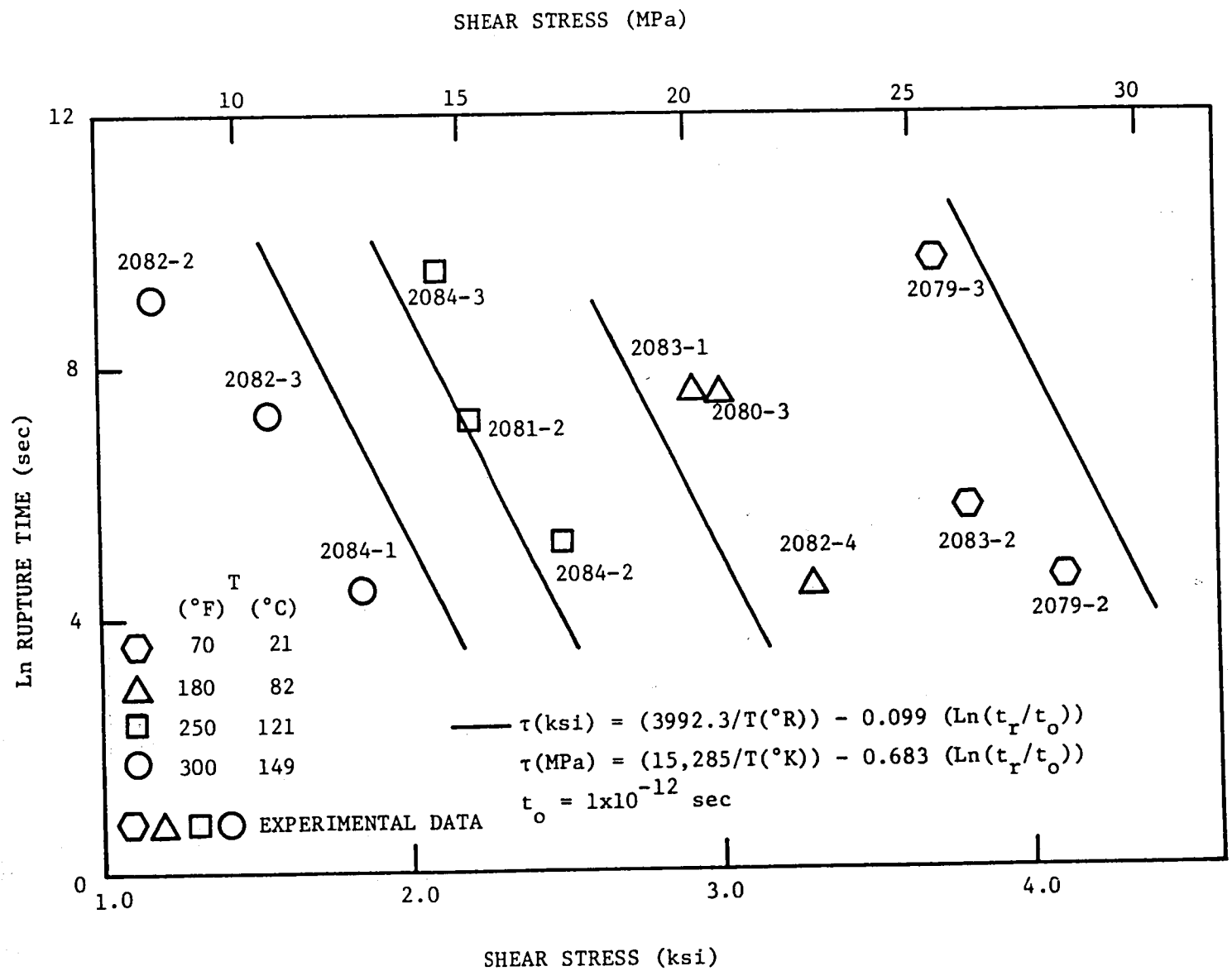

Figure 22. Creep Rupture Data and Comparison with Zhurkov's Equation for FM 300 Adhesive.

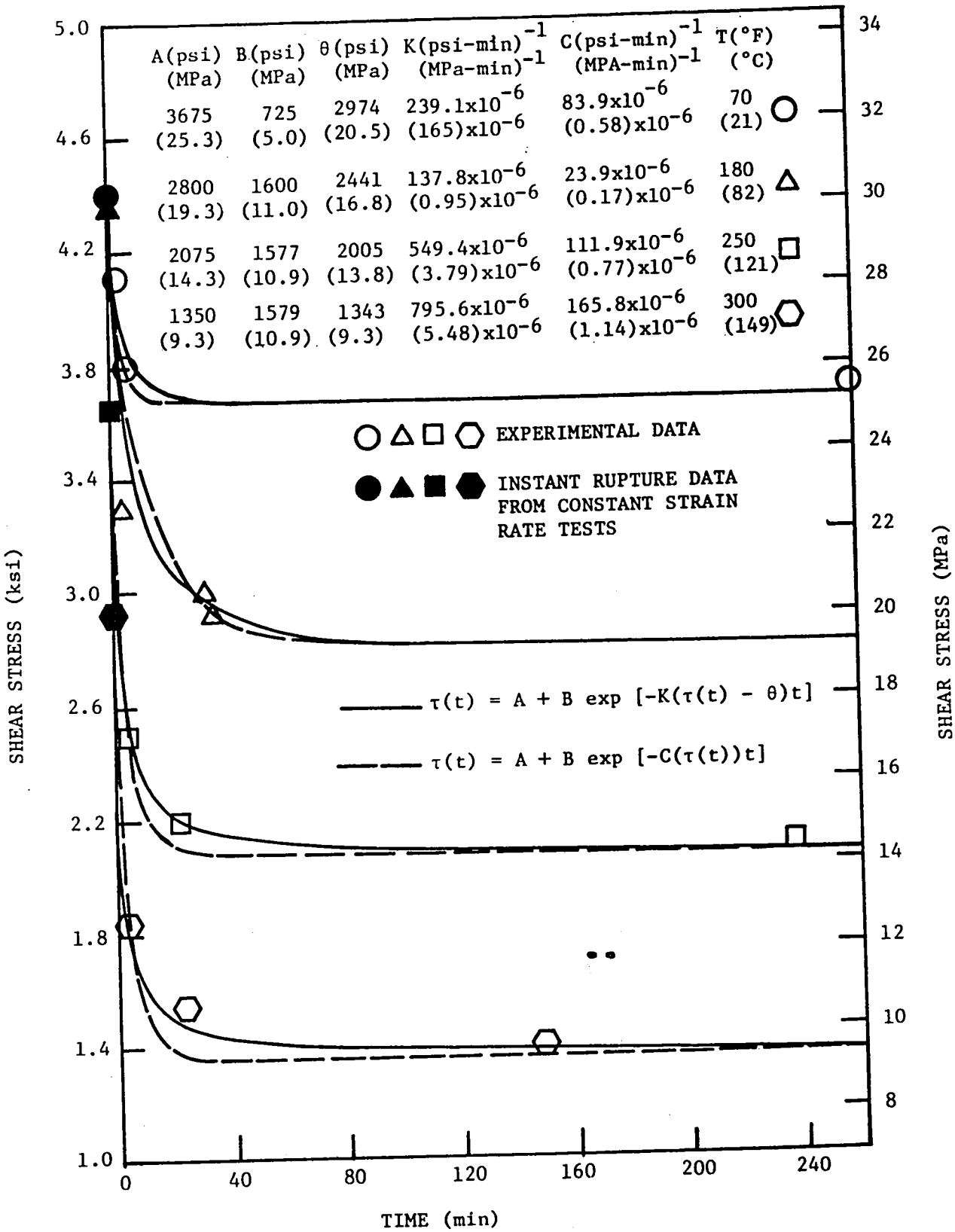

Figure 23. Creep Rupture Data and Comparison with Crochet's Equation for FM 300 Adhesive.

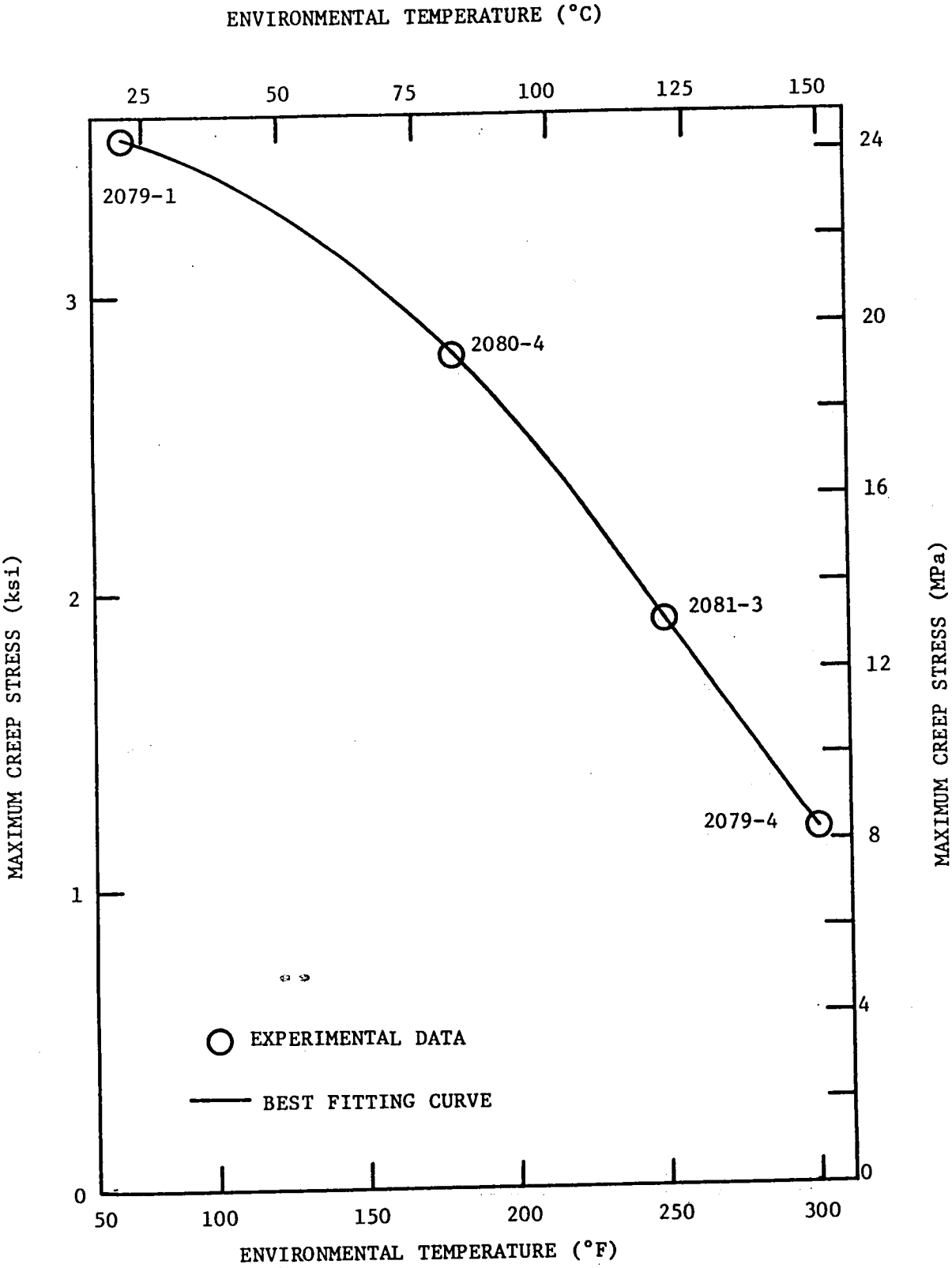

Figure 24. Variation of Maximum (Safe) Creep Stress with Environmental Temperature for FM 300 Adhesive.

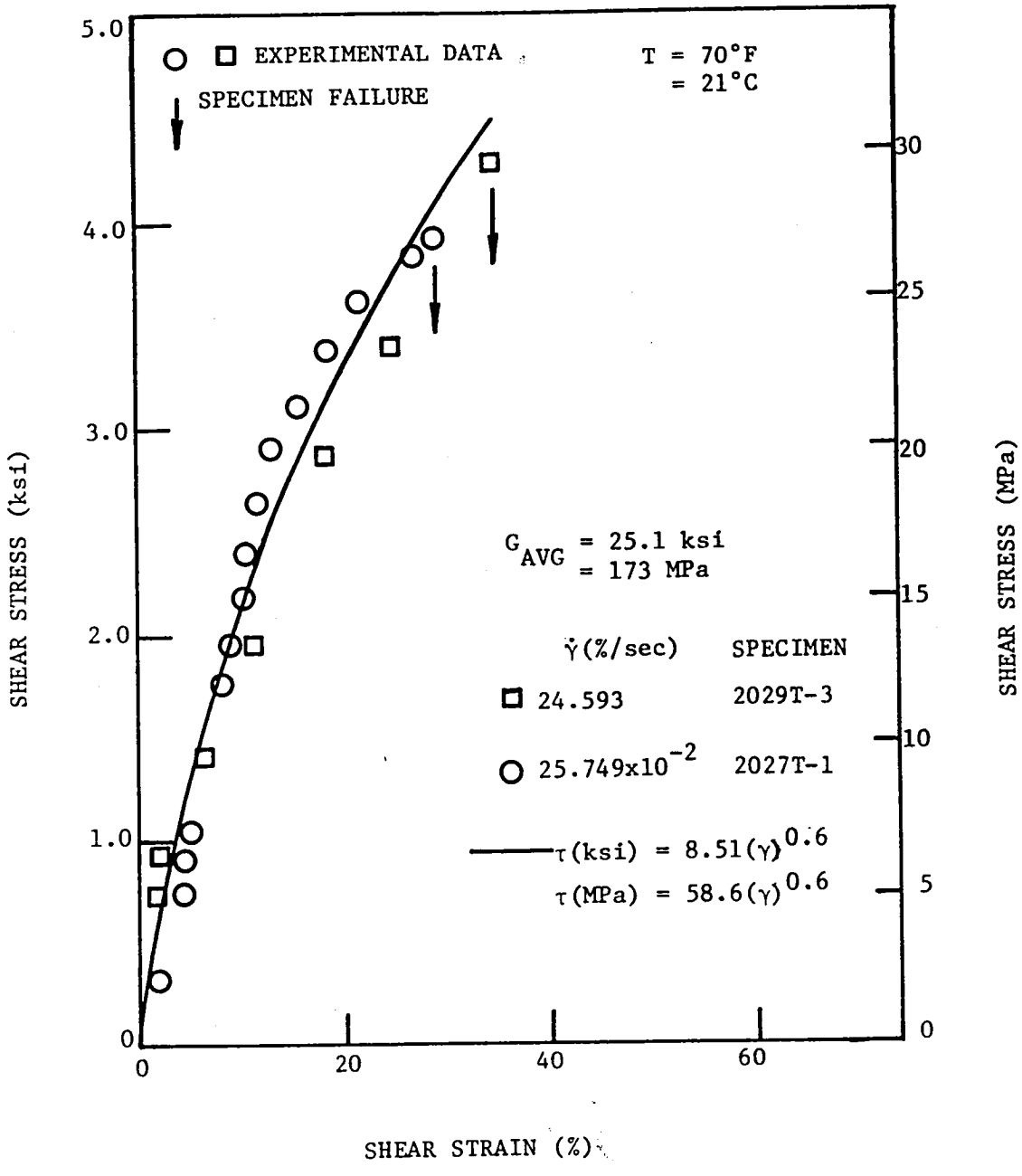

Figure 25. Constant Strain Rate Stress-Strain Behavior of Thermoplastic Polyimide-sulfone and Comparison with Theory.

mechanical behavior of the adhesive. The power law model, with the use of material constants shown, provides a good fit to the experimental data.

Figures 26 and 27, respectively, show the variation of the ultimate shear stresses and maximum shear strains with the initial elastic shear strain rate. Only an 8 % increase in the joint strength over a 100 times increase in the shear strain rate is observed (figure 26). The maximum shear strain data indicates a relatively constant value of maximum shear strains over a wide range of strain rates (figure 27). Figure 26 also shows Ludwik's equation fitted to the experimental data.

The constant strain rate shear stress-strain behavior of Thermoplastic Polyimidesulfone at elevated temperatures is shown in figure 28. In comparison to the room temperature condition, the ultimate shear stress is ~22 % lower at both the 250°F (121°C) and 350°F (177°C) conditions; and ~44 % lower at the 450°F (232°C) condition. It can also be observed that, excluding the 350°F (177°C) condition, the maximum shear strains decrease at elevated temperatures. Such a reduction in the levels of maximum shear strain can be attributed to a change in the failure mechanism (possibly from adhesive matrix to adhesive-fiber and/or adhesive-adherend interfacial) of the lap joint.

Room temperature creep results for Thermoplastic Polyimidesulfone are shown in figure 29. As can be observed, the adhesive's resistance to creep, especially in the primary and secondary creep regions, is characteristic of linear thermoplastics. Secondary creep rates are much lower than those for adhesives with comparable strength values.

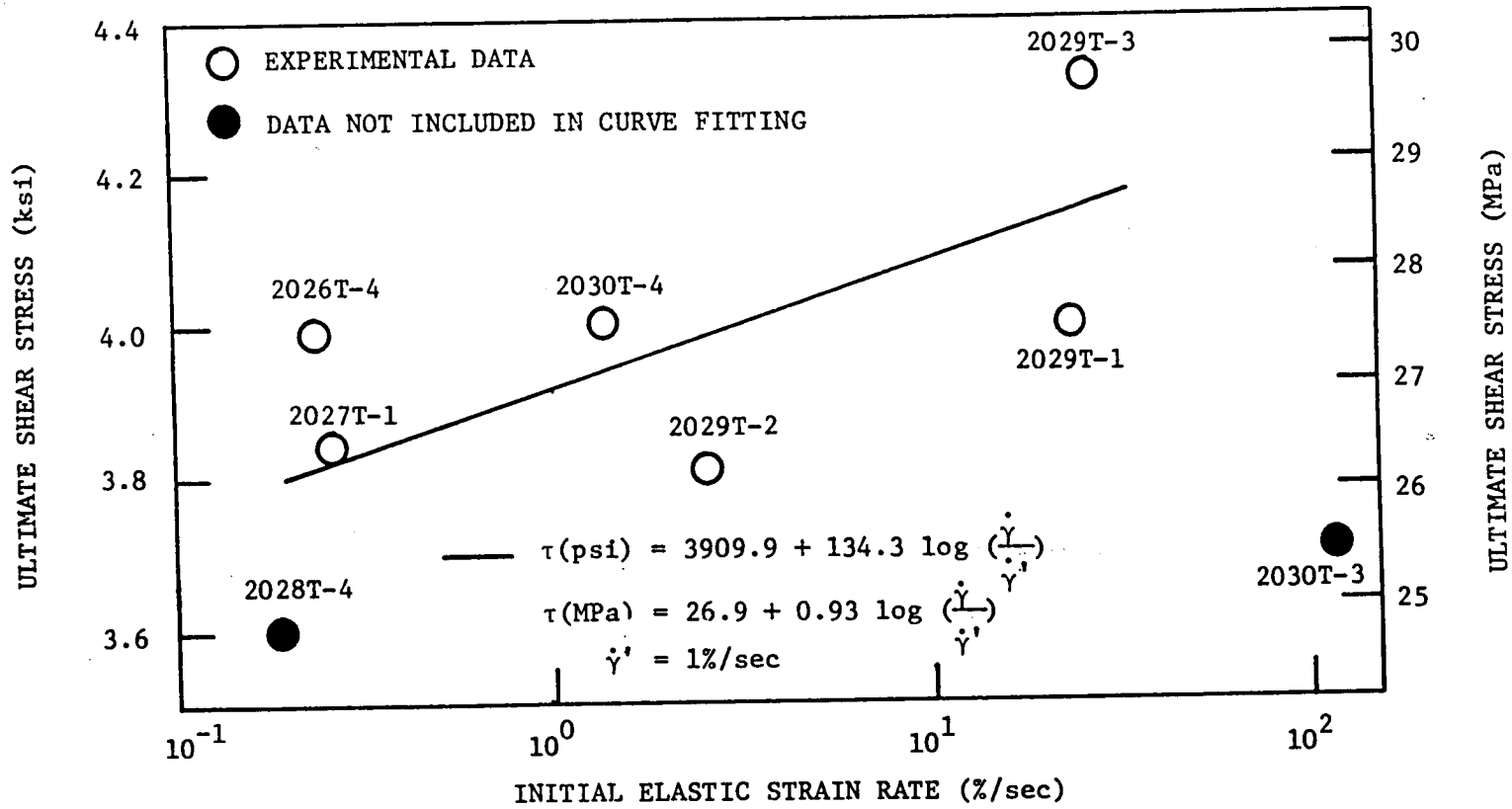

Figure 26. Variation of Ultimate Shear Stress with Initial Elastic Strain Rate and Comparison with Ludwik's Equation for Thermoplastic Polyimidesulfone Adhesive.

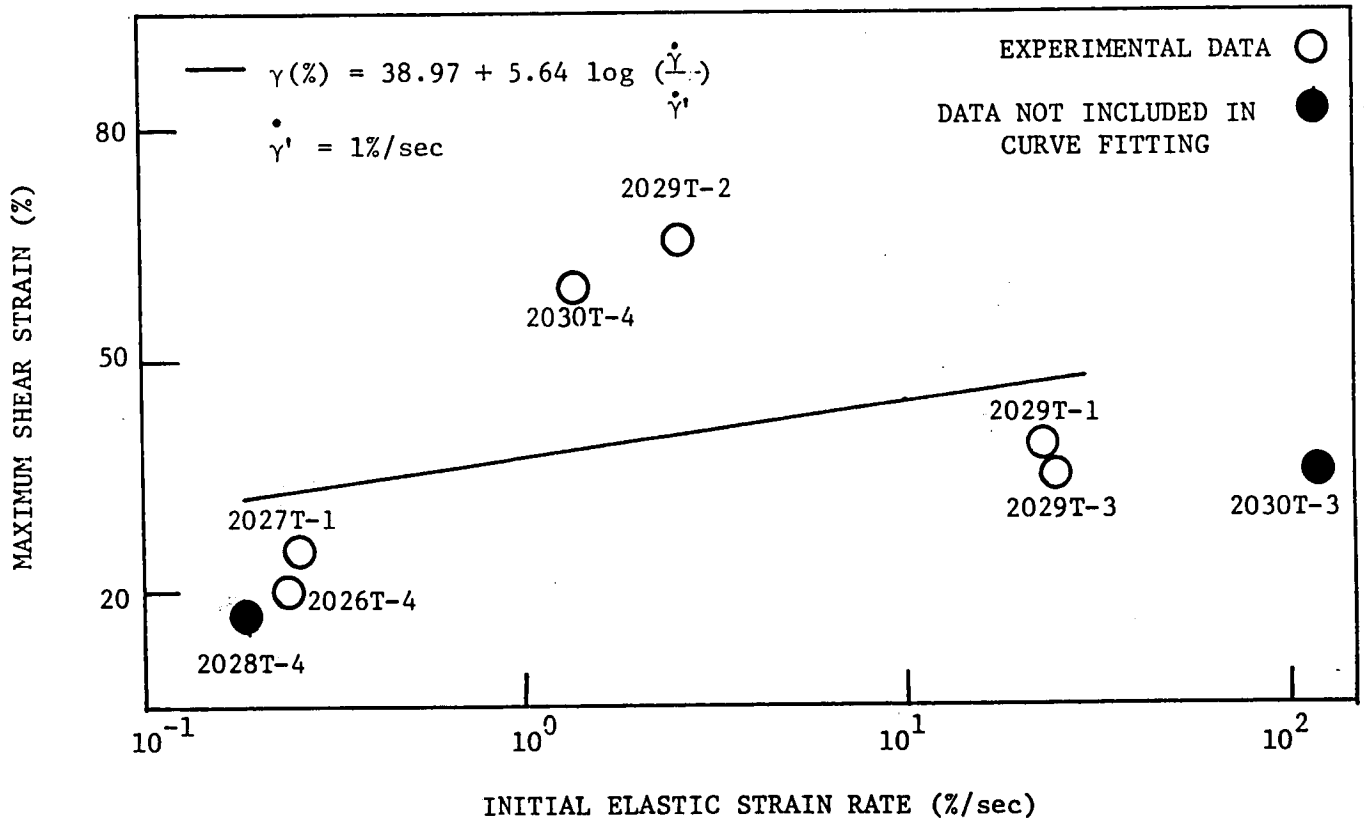

Figure 27. Variation of Maximum Shear Strain with Initial Elastic Strain Rate for Thermoplastic Polyimidesulfone Adhesive.

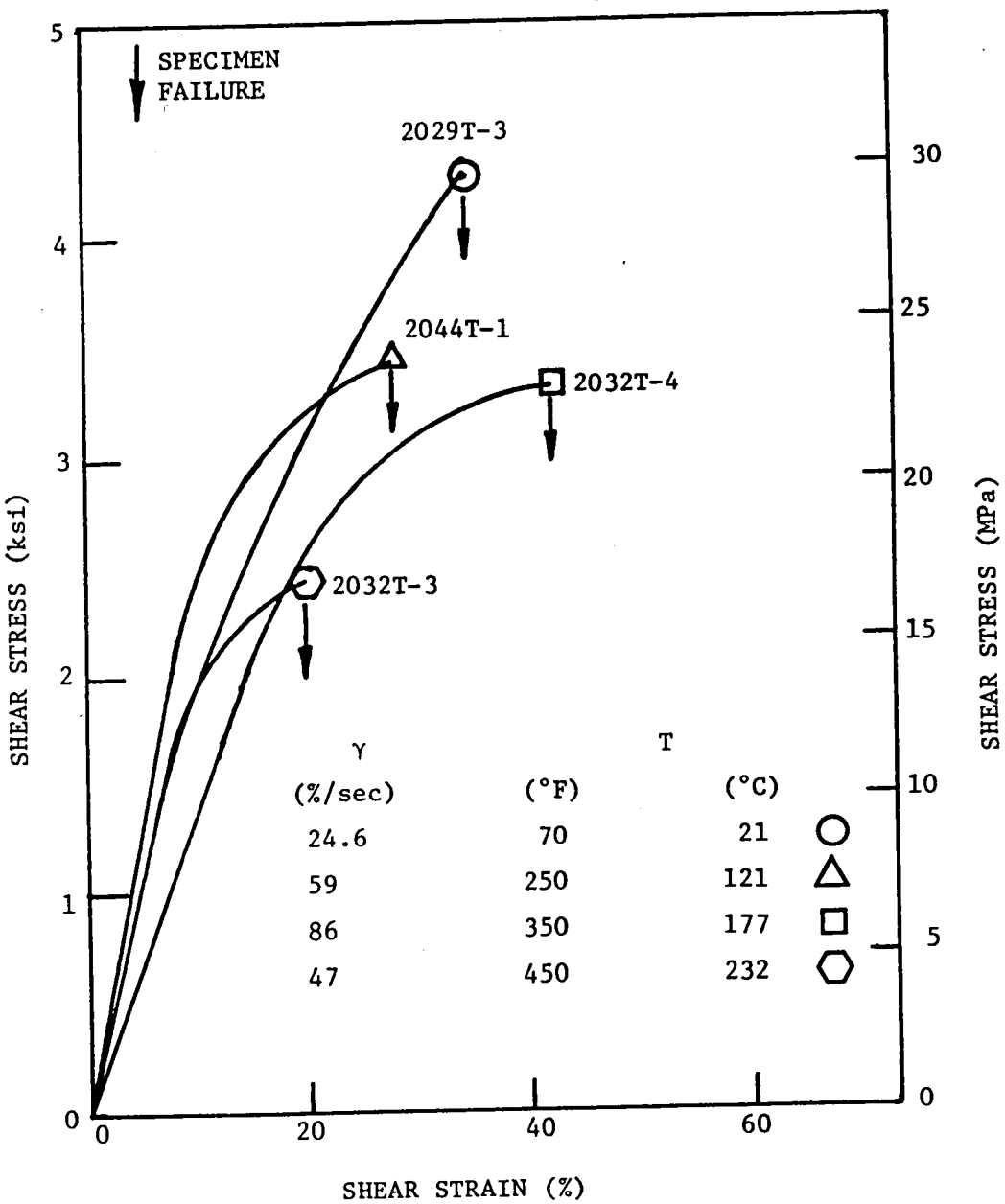

Figure 28. The Effects of Temperature on the Constant Strain Rate Stress-Strain Behavior of Thermoplastic Polyimide-sulfone Adhesive.

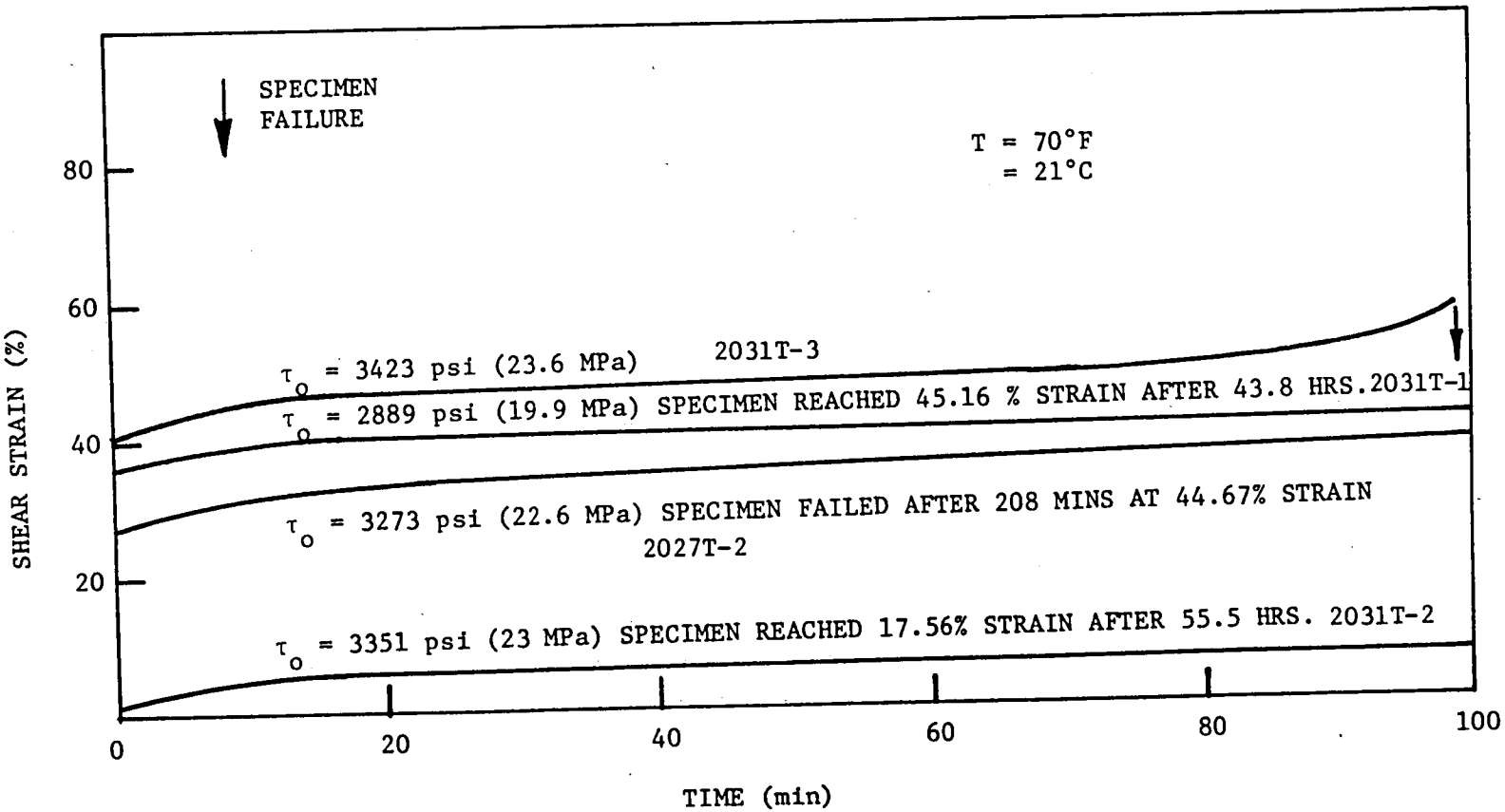

Figure 29. Room Temperature Creep Response of Thermoplastic Polyimidesulfone Adhesive.

The presence of a tertiary creep region is evident. It should also be noted that the level of initial shear strain (γ_o) reached for a given level of shear stress appears to control the oncoming creep process (compare creep behavior at 3273 psi - 22.6 MPa and, 3351 psi - 23 MPa).

The creep results of Thermoplastic Polyimidesulfone at 250°F (121 °C), 350°F (177°C) and 450°F (232°C) conditions are shown in figures 30, 31 and 32, respectively. A decrease in the levels of creep strains is observed with increasing temperatures, especially at the 450°F (232°C) condition where an almost constant level of shear strain is evident. The reason for such a decrease in the levels of shear strain becomes obvious when one examines the post-failure surfaces of the specimens (figure 33). The extent of interfacial separation, especially adhesive-adherend (and also adhesive-fiber) separation increases with an increase in the environmental temperature. The gradual darkening of the post-failure overlap areas with increasing temperatures (in figure 33) is an indication of adhesive matrix layers which have separated from the adherend and/or the carrier cloth. Consequently, interfacial separations result in failures without appreciable adhesive deformation.

Creep-rupture data for Thermoplastic Polyimidesulfone is shown in figures 34 and 35. Figure 34 shows the comparison of Zhurkov's (modified) equation (equation 7) with the experimental data. As may be observed, data and theory show poor agreement. The discrepancy between data and theory is greater at the room temperature and 450°F (232°C) conditions. The constants U_o and γ used to fit Zhurkov's equation to the creep-rupture data are also shown in figure 34.

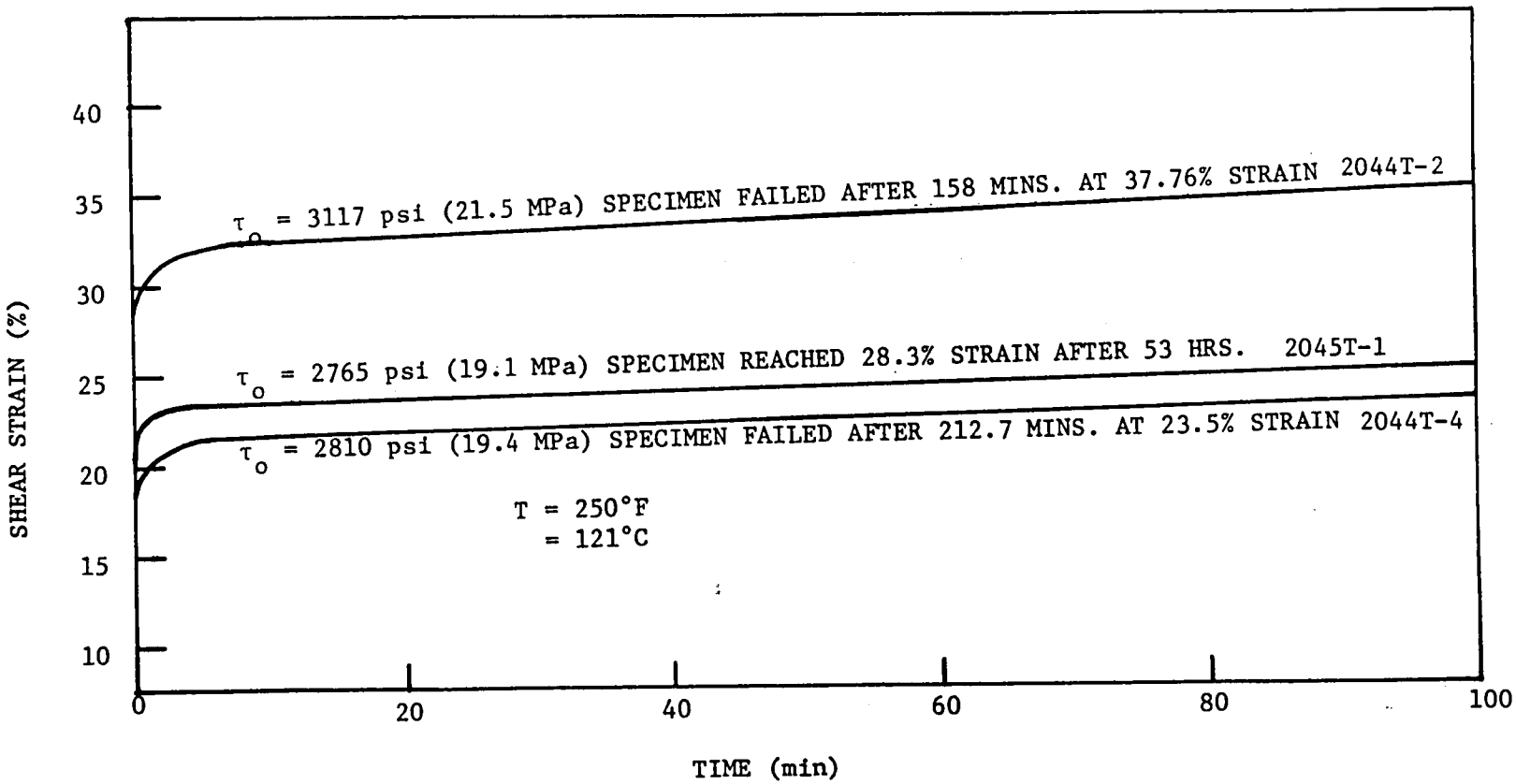

Figure 30. Creep Behavior of Thermoplastic Polyimidesulfone Adhesive at 250°F (121°C) Condition.

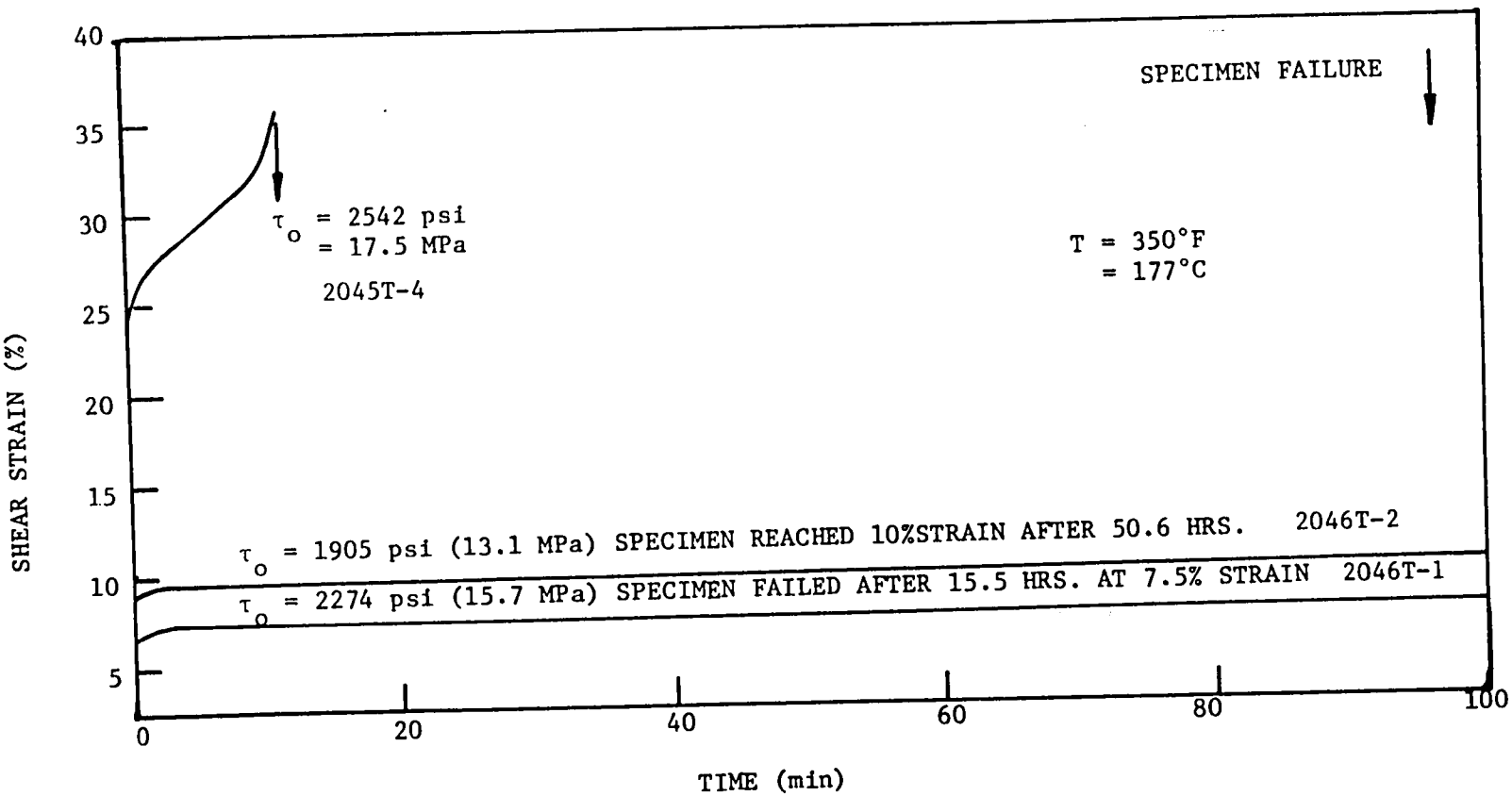

Figure 31. Creep Behavior of Thermoplastic Polyimidesulfone Adhesive at 350°F (177°C) Condition.

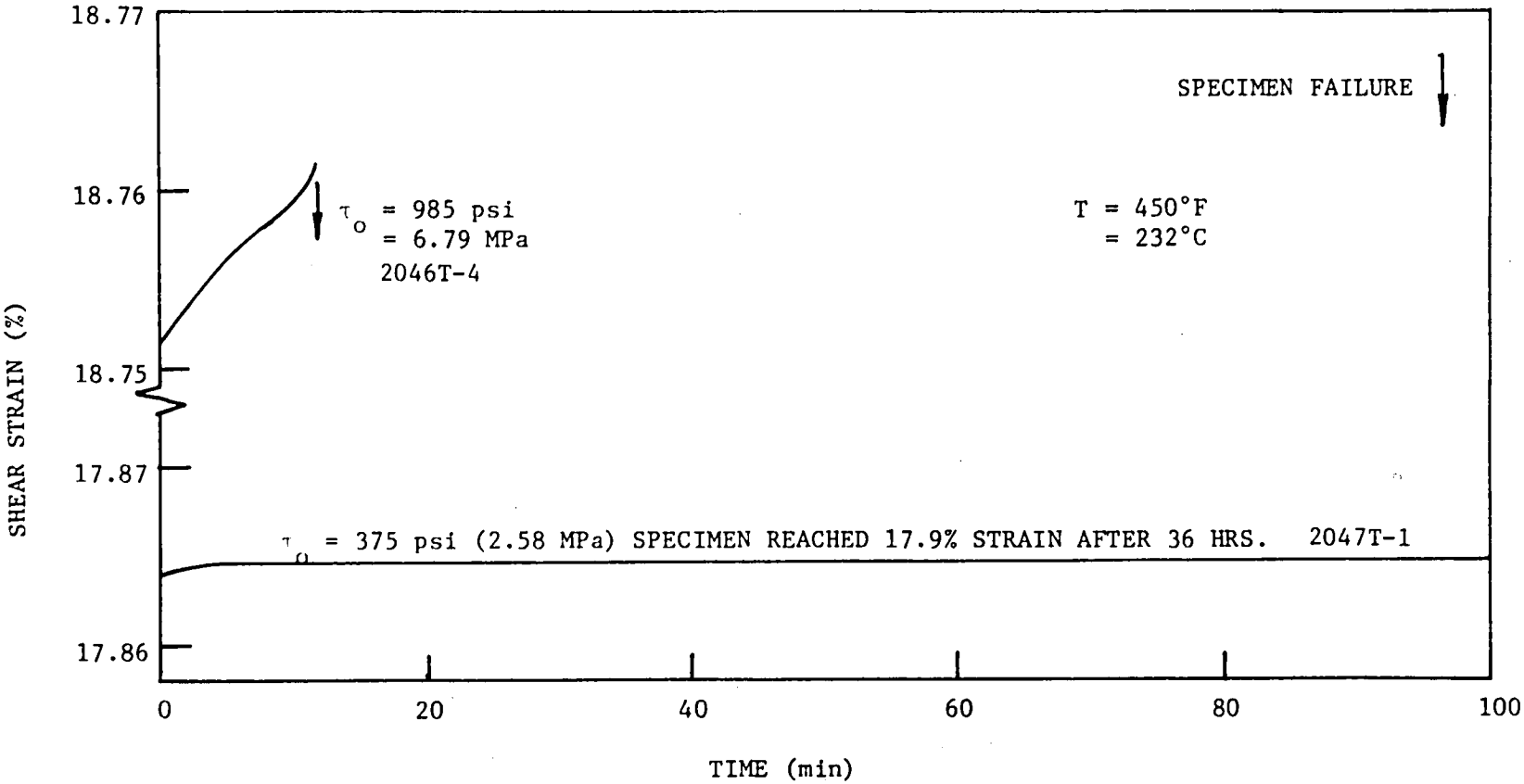

Figure 32. Creep Behavior of Thermoplastic Polyimidesulfone Adhesive at 450°F (232°C) Condition.

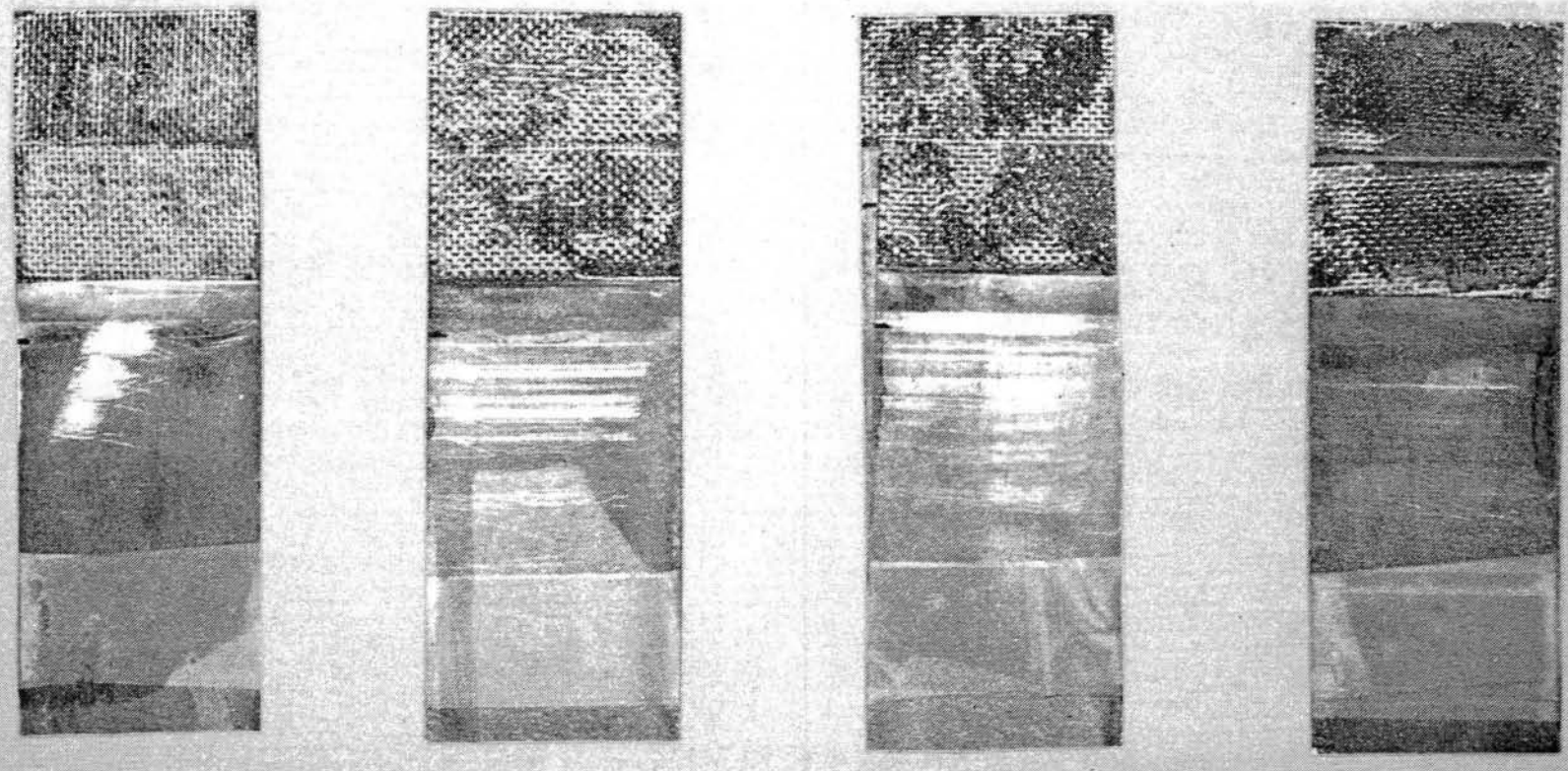

T = 70°F = (21°C)

T = 250°F = (121°C)

T = 350°F = (177°C)

T = 450°F = (232°C)

Figure 33. Typical Fracture Surfaces of Titanium-Polyimidesulfone Specimens Exhibiting the Effects of Increasing Temperature.

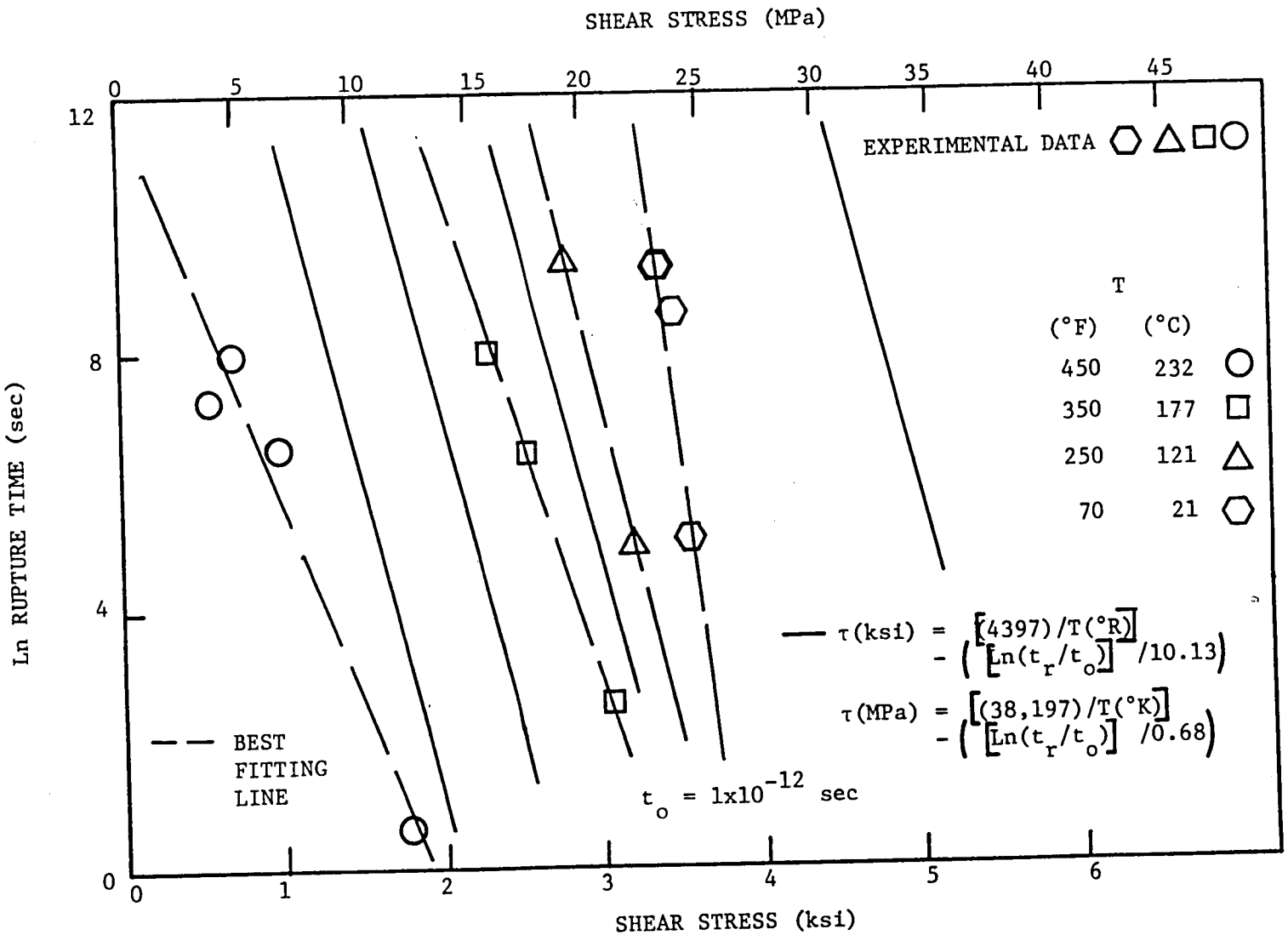

Figure 34. Creep Rupture Data and Comparison with Zhurkov's Equation for Thermoplastic Polyimidesulfone Adhesive.

Figure 35 shows the comparison of creep-rupture data with Crochet's equation (equation 10) based on the Maxwell model. Apparently, Crochet's equation provides a better fit to the experimental data in comparison to Zhurkov's equation. The appropriate constants used in fitting Crochet's equation (based on the Maxwell model) to the creep-rupture data are also shown in figure 35.

Figure 36 shows variation of the maximum -or safe- level of creep stress values(below which creep failures are not expected to occur) with environmental temperature. The maximum creep stress values represent the asymptotic shear stress levels (i.e. material constants A in figure 35) obtained with the application of Crochet's equation. A sharp decrease in the level of maximum creep stress is observed for temperatures above 350°F (177°C).

A comparison of the mechanical properties of FM 73, FM 300 and Thermoplastic Polyimidesulfone adhesives at comparable testing conditions is shown in Table 1 (page 66). As may be observed from Table 1, the epoxy adhesives, FM 73 and FM 300, are clearly inferior to the polyimide adhesive, Thermoplastic Polyimidesulfone, in high temperature strength retention. The creep resistance of the polyimide adhesive is higher than that for the epoxy adhesives, especially at elevated temperatures.

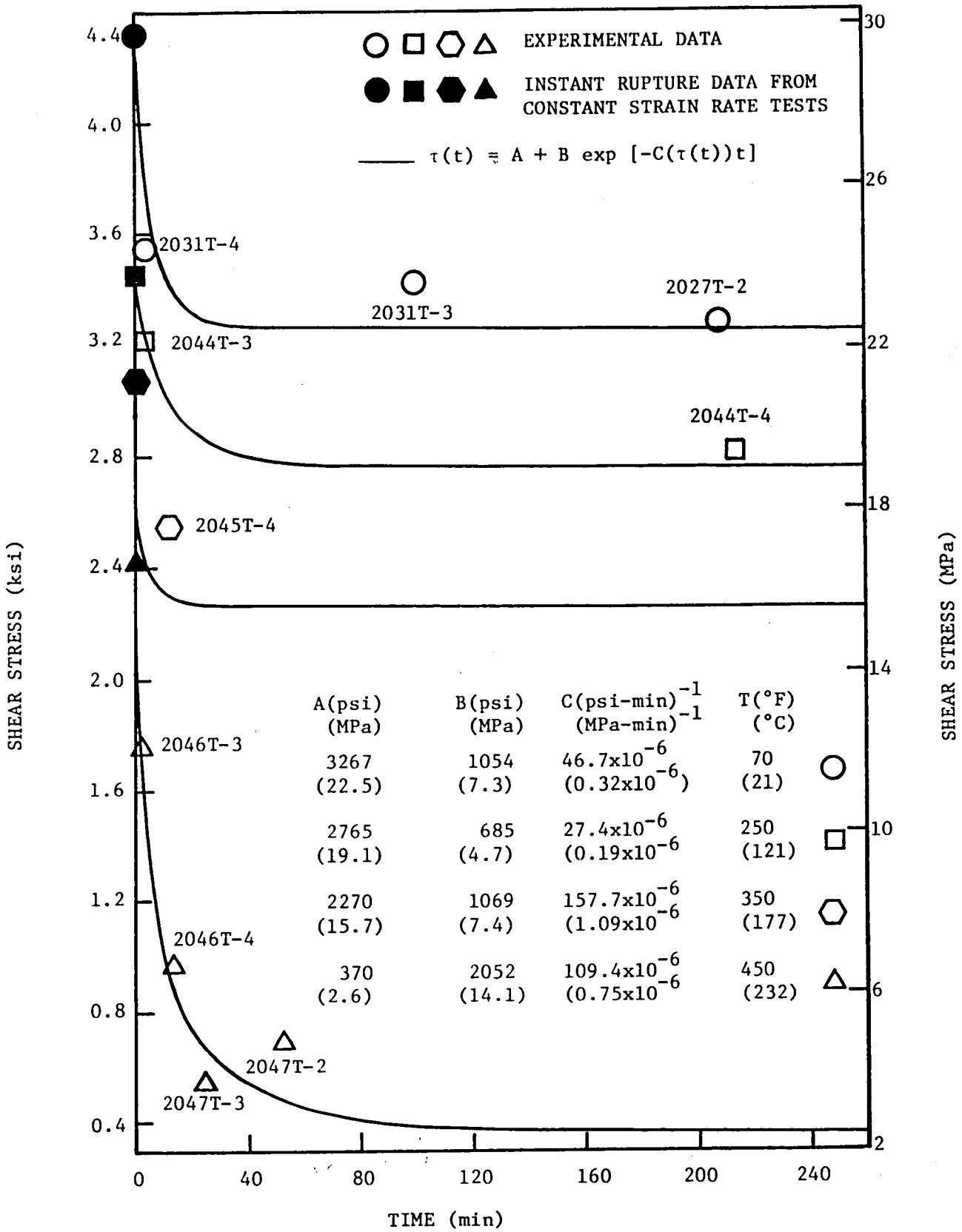

Figure 35. Creep Rupture Data and Comparison with Crochet's Equation for Thermoplastic Polyimidesulfone Adhesive.

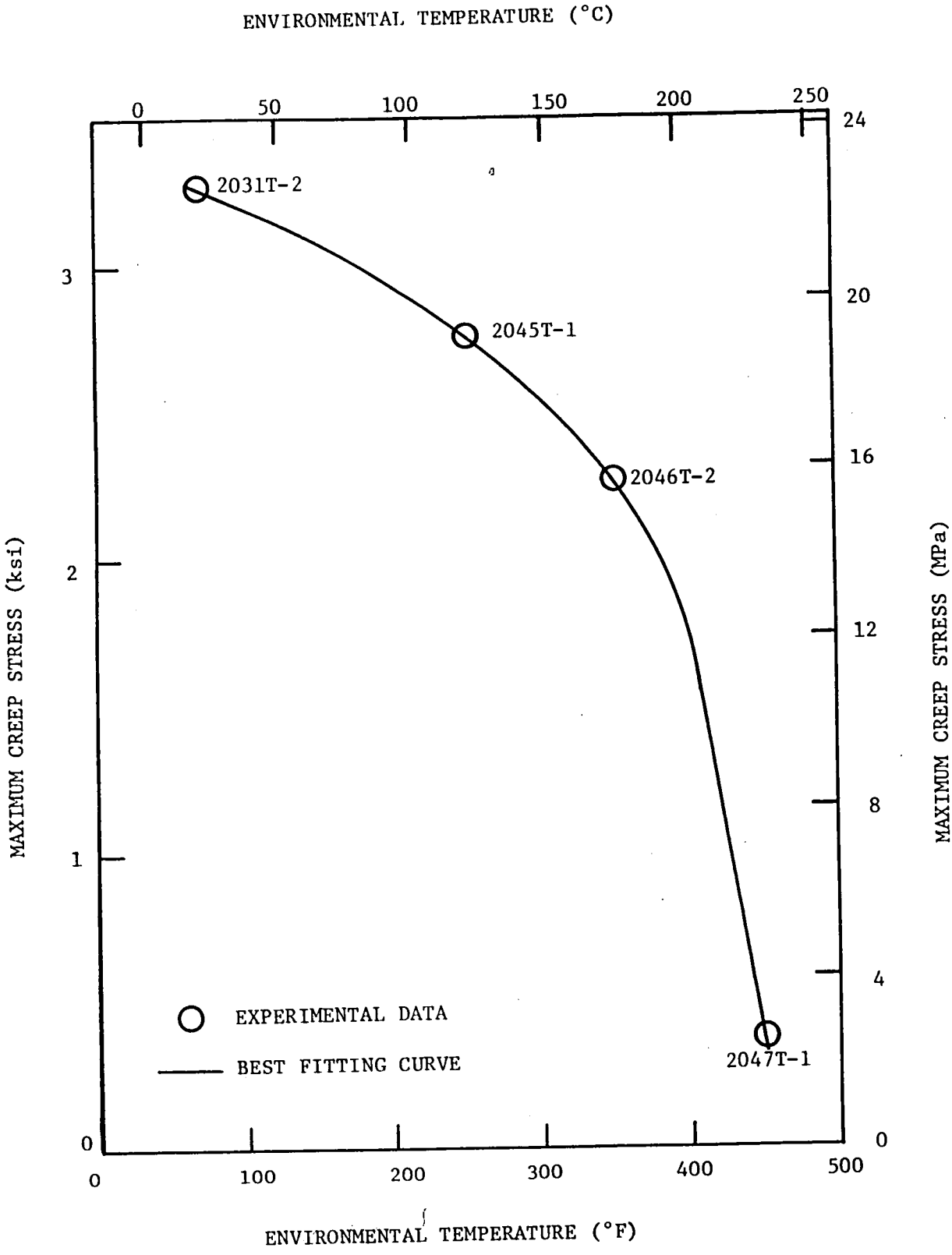

Figure 36. Variation of Maximum (safe) Creep Stress with Environmental Temperature for Thermoplastic Polyimidesulfone Adhesive.

Property and Test Condition	FM 73 Adhesive	FM 300 Adhesive	Thermoplastic Polyimidesulfone
Elastic Shear Modulus, G T=70°F (21°C)	12.7 ksi (87.6 MPa)	19.7 ksi (136.1 MPa)	25.1 ksi (173.0 MPa)
Maximum Shear Stress and Strain Under Constant Strain Rate Conditions at 70°F (21°C)	3,469 psi (23.9 MPa) 58.5 % (0.75 %/sec)	4,300 psi (29.7 MPa) 31.2 % (1.94 %/sec)	3,947 psi (27.2 MPa) 59.6 % (1.35 %/sec)
Maximum Shear Stress and Strain Under Constant Strain Rate Conditions at 250°F (121°C)	500 psi (3.45 MPa) 107 % (2.36 %/sec)	3,652 psi (25.2 MPa) 72.8 % (384 %/sec)	3,450 psi (23.8 MPa) 37.5 % (59.1 %/sec)
Room Temperature Creep Strain at Comparable Creep Stresses	85.25 % 3,499 psi (24.1 MPa)	32.01% 3,535 psi (24.4 MPa)	56.76 % 3,423 psi (23.6 MPa)
Maximum Creep Strain at 180°F (82°C)	130 % 1,104 psi (7.6 MPa)	65 % 2,925 psi (20.2 MPa)	----- ----- (-----)
Maximum Creep Strain at 250°F (121°C)	----- ----- (-----)	125 % 2,200 psi (15.2 MPa)	37.76 % 3,117 psi (21.5 MPa)
Maximum (Safe) Level of Creep Stress at 70°F (21°C)	3,097 psi (21.4 MPa)	3,675 psi (25.3 MPa)	3,267 psi (22.5 MPa)
Maximum (Safe) Level of Creep Stress at 180°F (82°C)	982 psi (6.8 MPa)	2,800 psi (19.3 MPa)	----- (-----)
Maximum (Safe) Level of Creep Stress at 250°F (121°C)	----- (-----)	2,075 psi (14.3 MPa)	2,765 psi (19.1 MPa)

Table 1. Mechanical Properties of FM 73, FM 300 and Thermoplastic Polyimidesulfone Adhesives at Comparable Testing Conditions.

CHAPTER 5

CONCLUSIONS

The present investigation was concerned with the development of a practical method for characterizing structural adhesives in the bonded lap shear mode. The validity of this proposed characterization method was evaluated with the use of experimental constant strain rate, creep and creep-rupture data. Three different model adhesives were used in the bonded lap shear mode for this purpose. Elevated temperature behavior was also studied.

Based on the experimental data from the three adhesives studied, the following conclusions can be made:

1) It is possible to describe the constant strain rate shear stress-strain behavior of structural adhesives in the bonded form by using viscoelastic or nonlinear elastic relations.

2) Ludwik's equation provides an adequate description of the rate dependent ultimate and elastic limit shear stresses.

3) Crochet's equation provides a better description of the temperature dependent creep-rupture data in comparison to Zhurkov's equation.

4) The epoxy adhesives, FM 73 and FM 300, are clearly inferior to the polyimide adhesive, Thermoplastic Polyimidesulfone, in high temperature strength retention.

The authors' suggestions for future work include correlation of bulk adhesive properties to single lap shear data. The effects of temperature on the rate dependent behavior and viscosity of adhesives

should also be studied as a continuation of the present investigation. Results from such a study can be correlated to those from the constant strain rate tests conducted at elevated temperatures herein. Future efforts in the study of the effects of polymer molecular weight on adhesive mechanical behavior should also prove to be worthwhile.

REFERENCES

1. Brinson, H.F., "The Viscoelastic-Plastic Characterization of a Ductile Polymer," Deformation and Fracture of High Polymers, H. Kaush et. al., eds., Plenum Press, NY, 1974.

2. Brinson, H.F., Renieri, M.P., and Herakovich, C.T., "Rate and Time Dependent Failure of Structural Adhesives," Fracture Mechanics of Composites, ASTM STP 593, 1975, pp. 177-199.

3. Sancaktar, E. and Brinson, H.F., "The Viscoelastic Shear Behavior of a Structural Adhesive," Adhesion and Adsorption of Polymers, 12-A, Plenum Publishing Corp., 1980.

4. Chase, K.W. and Goldsmith, W., "Mechanical and Optical Characterization of an Anelastic Polymer at Large Strain Rates and Strain," Experimental Mechanics, p. 10, Jan. 1974.

5. Sancaktar, E. and Padgilwar, S., "The Effects of Inherent Flaws on the Time and Rate Dependent Failure of Adhesively Bonded Joints," Transactions of the ASME Journal of Mechanical Design, Vol. 104, No. 3, pp. 643-650, (1982).

6. Thorkildsen, R.L., Engineering Design for Plastics, E. Baer (Ed.), Reinholt Book Co., New York (1964), p. 295.

7. Zhurkov, S.N., "Kinetic Concept of the Strength of Solids," Internl. J. of Frac. Mech., 1 (4), 331-323 (1965).

8. Crochet, M.J., "Symmetric Deformations of Viscoelastic-Plastic Cylinders," J. of Appl. Mech., 33, p.326, 1966.

9. Bugel, T.E., Norwalk, S. and Snedeker, R.H., "Phenoxy Resin - A New Thermoplastic Adhesive," Adhesion, Ed. Eley, D.D., pp. 87-94, Oxford University Press, 1961.

10. St. Clair, T.L. and Yamaki, D.A., "A Thermoplastic Polyimide-sulfone," NASA Langley Research Center, Technical Memorandum No. 84574, Nov. 1982.

11. FM 73 Adhesive Film Product Information Brochure. American Cyanamid Company, Bloomingdale Products, Havre de Grace, Maryland 21078.

12. FM 300 Adhesive Film Product Information Brochure. American Cyanamid Company, Bloomingdale Products, Havre de Grace, Maryland 21078.

13. Goland, M. and Reissner, E., "The Stresses in Cemented Joints," J. Applied Mechanics, Vol. II, No. 1, March 1944.

14. Mall, S., Johnson, W.S. and Everett, R.A., Jr., "Cyclic Debonding of Adhesively Bonded Composites," NASA Langley Research Center, Technical Memorandum No. 84577, Nov. 1982.

15. Nadai, A. and Manjoine, M.J., Journal of Applied Mechanics, vol. 8, p. A82, 1941.

16. Slonimskii, G.L., Askadskii, A.A. and Kazantseva, V.V., "Mechanism of Rupture of Solid Polymers," Polymer Mech., 5 (1977).

17. Brinson, H.F., Griffith, W.I. and Morris, D.H., "Creep Rupture of Polymer-Matrix Composites," Experimental Mechanics, Sept. 1981, pp. 329-335.

18. Reiner, M., Advanced Rheology, H.K. Lewis and Co. Ltd., London, 208, 1971.

19. Schapery, R.A., "On the Characterization of Nonlinear Viscoelastic Materials," Poly. Eng. and Sci., Vol. 9, No. 4, July 1969, pp. 295-310.

20. Cartner, J.S. and Brinson, H.F., "The Nonlinear Viscoelastic Behavior of Adhesives and Chopped Fiber Composites," Virginia Polytechnic Institute Report No. VPI-E-78-21, August 1978.

21. Greenwood, L., "The Strength of a Lap Joint," Aspects of Adhesion, Vol. 5, 1969, pp. 40-50.

APPENDIX A

CALCULATION OF OVERLAP EDGE STRESS CONCENTRATION FACTORS.

The quantity reported as the "lap shear strength," is the breaking load per unit bond area. However, failure initiation in materials is a localized phenomenon that is dependent on the maximum stresses at a point reaching some critical value. The standard lap shear specimen shows a variation in the shear stress within the adhesive layer and, in fact, can exhibit a singular behavior at the bond termination.

Volkersen [21] analyzed the stress distribution in single lap joint geometry under a load due to stretching of the adherends while ignoring the tearing stresses at the free ends. He considered the case where two identical elastic adherends of uniform thickness, t and a Young's moduli of E, bonded over a length of 2C by an adhesive of thickness m which was assumed to behave like an elastic solid with shear modulus G_a. The bonded faces of the adherends were assumed to be parallel so that the thickness m was considered constant. Volkersen's analysis showed that when the bonded members are in pure tension, the shear stress in the adhesive layer is a maximum at each end of the overlap. He compared the maximum shearing stress at the end of the overlap with the mean stress to evaluate the stress concentration factor,

$$n_v = \sigma' \coth(\sigma') \tag{24}$$

where

$$\sigma' = [(2C^2 G_a)/(Etm)]^{1/2} \tag{25}$$

Goland and Reissner [13], in their analysis of the single lap joint geometry, showed the existence of high stress concentrations near each end of the overlap region, in the form of peak normal (tearing) and shear adhesive stresses. The magnitudes of these stresses depend on

1) the flexibility of the adhesive,

2) the length of overlap,

3) Young's moduli of the adherends,

4) the thickness of the adherends, and

5) the thickness of the adhesive layer.

Goland and Reissner categorized adhesively bonded joints into two approximate groups to simplify their analysis.

In the first approximation, the work of the normal (σ_o) and shear (τ_o) adhesive stresses were neglected in comparison to the work of the adherend stresses (σ_y and τ_{xy}) which were assumed to be continuous across the adhesive layer. Adhesive layers were considered inflexible for joints satisfying the conditions

$$(m/E) << (t/E),\ (m/G) << (t/G). \tag{26}$$

In the second approximation, the work of the adherend stresses was ignored in comparison to the work of adhesive stresses σ_y and τ_{xy}, for joints satisfying the conditions

$$(m/E) >> (t/E) \text{ or } (m/G) >> (t/G). \tag{27}$$

Such joints were considered to have flexible adhesive layers.

The single lap joints used for the present investigation can be considered to have flexible adhesive layers. Based on the Goland and Reissner analysis [13], the stress concentration factor, n_{GR}, for flexible joints can be calculated as

$$n_{GR} = (1/4)[(BC/t)(1+3k)\coth(BC/t)+3(1-k)] \tag{28}$$

where

$$B = \sqrt{(8G_a t/Em)}\ , \tag{29}$$

$$k = (\cosh(UC))/(\cosh(UC)+2\sqrt{2\sinh(UC)}), \tag{30}$$

$$UC = \sqrt{[3(1-\nu^2)/2]}\ (C/t)[F/(tWE)]^{1/2} \tag{31}$$

and

$$Y = [6E_a t/Em]^{1/4} \tag{32}$$

also:

ν = poisson's ratio for the adherends (0.30)

F = load applied to the adherends

E_a = elastic modulus for the adhesive

m = adhesive layer thickness

W = width of the adherend.

It should be noted that this approach again neglects the presence of tearing stresses in the adhesive layer. A more accurate analysis should include the effect of the tearing stresses as described below.

Since both normal $(\sigma_o)_{max}$ and shear $(\tau_o)_{max}$ stresses exist at the overlap edge, principal (normal), σ_1 and maximum shear, τ_{max}, stresses need to be calculated for the assessment of the failure condition. These stresses can be calculated with the use of equations

$$\sigma_1 = (\sigma_o)_{max}/2 + [((\sigma_o)_{max}/2)^2 + ((\tau_o)_{max})^2]^{1/2} \quad (33)$$

and,

$$\tau_{max} = [((\sigma_o)_{max}/2)^2 + ((\tau_o)_{max})^2]^{1/2} \quad (34)$$

where $(\tau_o)_{max}$ is given by equation (28) and $(\sigma_o)_{max}$ is determined by the method of Goland and Reissner [13] as

$$(\sigma_o)_{max} = (F/tW)(C/t)^2[(L^2k/2)(\sinh(2L)-\sin(2L))/(\sinh(2L)+\sin(2L)) + Lk'(\cosh(2L)+\cos(2L))/(\sinh(2L)+\sin(2L))] \quad (35)$$

where

$$L = (YC/t), \quad (36)$$

$$k' = (V_oCW/Ft), \quad (37)$$

and,

$$V_o = (kF/W)[3F(1-\nu^2)/(tEW)]^{1/2} \quad (38)$$

More accurate stress concentration factors n_τ and n_σ, can now be calculated by dividing τ_{max} and σ_1 respectively by the average shear stress ($\tau = F/A$).

Application of the four methods discussed above for calculating the stress concentration factor, n, for single lap joints bonded with FM 73, FM 300 and Thermoplastic Polyimidesulfone adhesives under constant strain rate loading yields the following results:

Adhesive	Specimen	n_ν	n_{GR}	n_τ	n_σ
FM 73	SJ-9-4	1.8828	2.4552	2.7458	3.9752
	SJ-10-2	2.1493	2.8000	3.1404	4.5404
FM 300	2078-3	2.0283	2.6549	2.9721	4.3081
	2083-3	2.0017	2.6264	2.9404	4.2626
	2078-2	1.9937	2.6126	2.9242	4.2376
	2083-4	1.8189	2.4305	2.7164	3.9295
Thermoplastic	2027T-1	2.3917	3.0312	3.4023	4.9476
Polyimidesulfone	2029T-3	2.3684	3.0296	3.3992	4.9408

where for

FM 73 adhesive

E_a = 337,068.87 psi [14]

ν = 0.40 [14],

FM 300 adhesive

E_a = 337,068.87 psi [14]

ν = 0.40 [14]

and,

Thermoplastic Polyimidesulfone

E_a = 719,000 psi [10]

ν = 0.38 [10].

APPENDIX B

TABLES OF SINGLE LAP SPECIMEN DIMENSIONS

TABLE B-2

Dimensions for Single Lap Specimens Bonded with FM 73 Adhesive.			
Specimen No.	Bondline Thickness Inches (CM)	Overlap Length Inches (CM)	Overlap Width Inches (CM)
SJ-5-1	0.00540(0.01372)	0.51969(1.32001)	0.99402(2.52481)
SJ-5-2	0.00470(0.01194)	0.52362(1.32999)	0.99410(2.52501)
SJ-5-3	0.00480(0.01219)	0.51969(1.32001)	0.99420(2.52527)
SJ-5-4	0.00520(0.01321)	0.53150(1.35001)	0.99475(2.52667)
SJ-6-2	0.00550(0.01397)	0.50886(1.29250)	0.99783(2.53449)
SJ-6-4	0.00740(0.01880)	0.50689(1.28750)	0.99616(2.53025)
SJ-7-1	0.00460(0.01168)	0.51083(1.29751)	0.99700(2.53238)
SJ-7-2	0.00500(0.01270)	0.51280(1.30251)	0.99050(2.51587)
SJ-7-3	0.00480(0.01219)	0.51870(1.31750)	0.98885(2.51168)
SJ-7-4	0.00480(0.01219)	0.52264(1.32751)	0.98850(2.51079)
SJ-8-1	0.00519(0.01318)	0.51969(1.32001)	0.99140(2.51816)
SJ-8-3	0.00501(0.01273)	0.51772(1.31501)	0.99265(2.52133)
SJ-9-2	0.00500(0.01270)	0.51969(1.32001)	0.99409(2.52499)
SJ-9-3	0.00550(0.01397)	0.51870(1.31750)	0.99499(2.52600)
SJ-9-4	0.00650(0.01651)	0.51673(1.31249)	0.99595(2.52971)
SJ-10-1	0.00540(0.01372)	0.53150(1.35001)	0.99675(2.53175)
SJ-10-2	0.00480(0.01219)	0.52559(1.33500)	0.99425(2.52540)
SJ-10-3	0.00474(0.01204)	0.52067(1.32250)	0.99270(2.52146)
SJ-10-4	0.00593(0.01506)	0.51378(1.30500)	0.99240(2.52070)

TABLE B-3

Dimensions for Single Lap Specimens Bonded with Thermoplastic Polyimidesulfone Adhesive.			
Specimen No.	Bondline Thickness Inches (CM)	Overlap Length Inches (CM)	Overlap Width Inches (CM)
2026T-4	0.00998(0.02535)	0.50500(1.28270)	0.99500(2.52730)
2027T-1	0.00839(0.02131)	0.52580(1.33553)	0.98540(2.50292)
2027T-2	0.00775(0.01969)	0.52006(1.32095)	0.98700(2.50700)
2028T-4	0.00970(0.02464)	0.53800(1.36652)	0.98100(2.49174)
2029T-1	0.00897(0.02278)	0.51400(1.30556)	0.98500(2.50190)
2029T-2	0.00919(0.02334)	0.51500(1.30810)	0.98400(2.49936)
2029T-3	0.00840(0.02134)	0.52099(1.32331)	0.98600(2.50444)
2030T-3	0.00889(0.02258)	0.53481(1.35842)	0.98540(2.50292)
2030T-4	0.00987(0.02507)	0.53684(1.36357)	0.98540(2.50292)
2031T-1	0.00869(0.02207)	0.52400(1.33096)	0.99100(2.51714)
2031T-2	0.00796(0.02022)	0.52500(1.33350)	0.98900(2.51206)
2031T-3	0.00797(0.02024)	0.52900(1.34366)	0.99400(2.52476)
2032T-3	0.00909(0.02309)	0.52710(1.33883)	0.97913(2.48699)
2032T-4	0.00894(0.02271)	0.53144(1.34986)	0.97125(2.46698)
2044T-1	0.01021(0.02593)	0.52953(1.34501)	0.98450(2.50063)
2044T-2	0.00983(0.02497)	0.52953(1.34501)	0.98455(2.50076)
2044T-3	0.00952(0.02418)	0.53642(1.36251)	0.98675(2.50635)
2044T-4	0.01058(0.02687)	0.53740(1.36500)	0.99315(2.52260)
2045T-1	0.01135(0.02883)	0.50787(1.28999)	0.99675(2.53175)
2045T-4	0.01094(0.02779)	0.50984(1.29499)	1.00300(2.54762)
2046T-1	0.00949(0.02410)	0.48819(1.24000)	0.99078(2.51658)
2046T-2	0.00871(0.02212)	0.50394(1.28001)	0.98980(2.51409)
2046T-3	0.00870(0.02210)	0.51378(1.30500)	0.98775(2.50889)
2046T-4	0.00859(0.02182)	0.52657(1.33749)	0.98675(2.50635)
2047T-1	0.01084(0.02753)	0.54134(1.37500)	0.99150(2.51841)
2047T-2	0.00895(0.02273)	0.53150(1.35001)	0.97750(2.48285)
2047T-3	0.00931(0.02365)	0.52362(1.32999)	0.97680(2.48107)

TABLE B-4

Dimensions for Single Lap Specimens Bonded with FM 300 Adhesive.			
Specimen No.	Bondline Thickness Inches (CM)	Overlap Length Inches (CM)	Overlap Width Inches (CM)
2078-2	0.00575(0.01460)	0.53346(1.35499)	0.99065(2.51625)
2078-3	0.00574(0.01458)	0.54230(1.37744)	0.98800 (2.50952)
2078-4	0.00644(0.01636)	0.54530(1.38506)	0.98800(2.50952)
2079-1	0.00678(0.01722)	0.52756(1.34000)	0.99225(2.52032)
2079-2	0.00596(0.01514)	0.52559(1.33500)	0.99075(2.51651)
2079-3	0.00647(0.01643)	0.51969(1.32001)	0.99050(2.51587)
2079-4	0.00612(0.01554)	0.51378(1.30500)	0.99150(2.51841)
2080-2	0.00629(0.01598)	0.53839(1.36751)	0.98800(2.50952)
2080-3	0.00594(0.01509)	0.53839(1.36751)	0.98650(2.50571)
2080-4	0.00657(0.01669)	0.53642(1.36251)	0.98575(2.50380)
2081-1	0.00524(0.01331)	0.52953(1.34501)	0.98250(2.49555)
2081-2	0.00535(0.01359)	0.53346(1.35499)	0.97925(2.48730)
2081-3	0.00503(0.01278)	0.53543(1.35999)	0.97775(2.48348)
2081-4	0.00491(0.01247)	0.53740(1.36500)	0.97825(2.48475)
2082-2	0.00592(0.01504)	0.53150(1.35001)	0.99000(2.51460)
2082-3	0.00601(0.01527)	0.52953(1.34501)	0.99000(2.51460)
2082-4	0.00588(0.01494)	0.52539(1.33449)	0.99325(2.52285)
2083-1	0.00611(0.01552)	0.54528(1.38501)	0.98975(2.51396)
2083-2	0.00516(0.01311)	0.53743(1.36507)	0.98775(2.50888)
2083-3	0.00562(0.01427)	0.52953(1.34501)	0.98375(2.49873)
2083-4	0.00647(0.01643)	0.51575(1.31001)	0.98975(2.51397)
2084-1	0.00501(0.01273)	0.54921(1.39499)	0.98475(2.50127)
2084-2	0.00588(0.01494)	0.55118(1.40000)	0.98650(2.50571)
2084-3	0.00573(0.01455)	0.55118(1.40000)	0.98950(2.51333)

1. Report No.	2. Government Accession No.	3. Recipient's Catalog No.
NASA CR-172237		

4. Title and Subtitle	5. Report Date
MATERIAL CHARACTERIZATION OF STRUCTURAL ADHESIVES IN THE LAP SHEAR MODE	September 1983
	6. Performing Organization Code

7. Author(s)	8. Performing Organization Report No.
Steven C. Schenck and Erol Sancaktar	
	10. Work Unit No.

9. Performing Organization Name and Address	11. Contract or Grant No.
Clarkson College of Technology Department of Mechanical and Industrial Engineering Potsdam, NY 13676	NAG1-284
	13. Type of Report and Period Covered
	Contractor Report

12. Sponsoring Agency Name and Address	14. Sponsoring Agency Code
National Aeronautics and Space Administration Washington, DC 20546	

15. Supplementary Notes Langley Technical Monitor: W. S. Johnson
Use of commercial products or names of manufacturers in this report does not constitute official endorsement of such products or manufacturers, either expressed or implied, by the National Aeronautics and Space Administration.

16. Abstract

A general method for characterizing structural adhesives in the bonded lap shear mode is proposed. Two approaches in the form of semi-empirical and theoretical approaches are used. The semi-empirical approach includes Ludwik's and Zhurkov's equations to describe respectively, the failure stresses in the constant strain rate and constant stress loading modes with the inclusion of the temperature effects. The theoretical approach is used to describe adhesive shear stress-strain behavior with the use of viscoelastic or nonlinear elastic constitutive equations. Three different model adhesives are used in the single lap shear mode with titanium adherends. These adhesives (one of which was developed at NASA Langley Research Center) are currently considered by NASA for possible aerospace applications. Use of different model adhesives helps in assessment of the generality of the method.

17. Key Words (Suggested by Author(s))		18. Distribution Statement
adhesive	creep rupture	Unclassified - Unlimited
visco-elastic	single lap specimen	
nonlinear-elastic	thermoplastic adhesive	Subject Category 27
rate effects	high temperature	
creep	Bingham model	

19. Security Classif. (of this report)	20. Security Classif. (of this page)	21. No. of Pages	22. Price
Unclassified	Unclassified	88	A05

For sale by the National Technical Information Service, Springfield, Virginia 22161